Chapter 6A

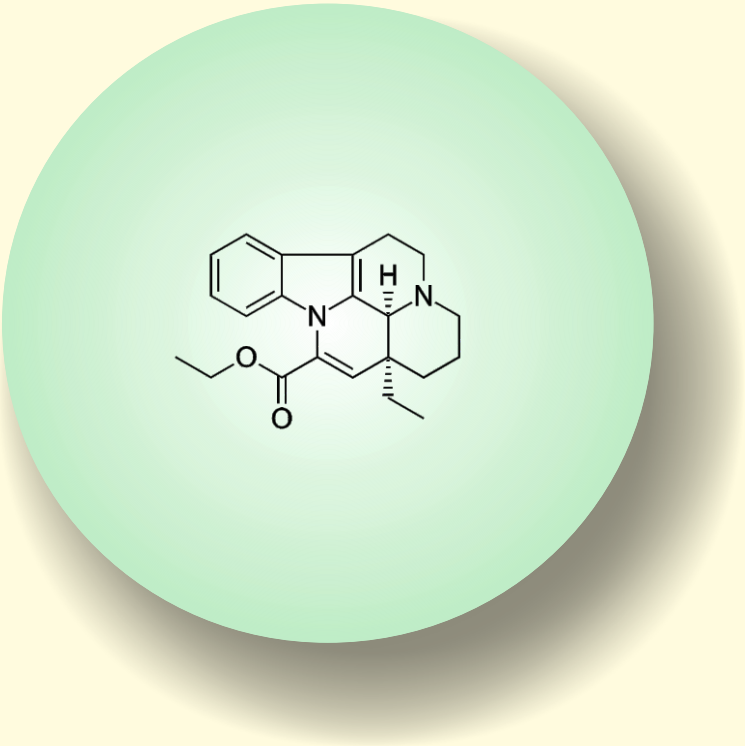

Formulation Development

Polymeric Nanoparticles

Vinpocetine

Contents

6A.1. INTRODUCTION

With an objective to achieve therapeutic plasma levels of VPN via transdermal route, polymeric nanoparticles (PNPs) were also developed. Ability of these nanocarriers to control the release of payload and ensure delivery in desired fashion have been widely reported in literatures [1]. Out of several available methods for preparation, the nanoprecipitation method was used [2]. A systematic quality-by-design (QbD) approach employing statistical design of experiments was utilized for optimization via establishing the impact of material attributes and process parameters on the critical formulation attributes [3].

6A.2. MATERIALS & METHODS

6A.2.1 Materials

Vinpocetine (VPN) was obtained as a gift sample from Covex S.A., Spain. PLGA 50:50 was kindly gifted by Purac Biomaterials, Netherlands. Poloxamer 188 was received from BASF, Ludwigshafen, Germany as gift

sample. Dialysis bags (MWCO, 12 kD) were purchased from HiMedia Labs Pvt. Ltd., Mumbai, India. Double distilled water was prepared in lab, filtered through 0.2μ membrane filter in glass bottle and consumed within a maximum of 7 days.

6A.2.2 Preparation of Vinpocetine loaded polymeric nanoparticles (VPN PNP)

Vinpocetine loaded PNP was prepared using nanoprecipitation method. Briefly, the VPN and PLGA were dissolved in acetone. A 5 ml of Poloxamer 188 solution was prepared in prefiltered distilled water and continuously stirred on a magnetic stirrer at room temperature. Then organic phase was slowly added into aqueous phase using a 1ml syringe. The stirring was continued for next 3-4 hours to allow complete evaporation of organic solvent. The PNP dispersion was centrifuged for 10 minutes at 5000 rpm and 15°C for the sedimentation of free drug. The supernatant nanoparticulate dispersion was carefully separated without disturbing the free drug pellet at the bottom. The separated nanoparticulate dispersion was stored in glass vials at 2-8°C till further analysis.

6A.2.2.1 Establishing Quality target product profile (QTPP) and Critical Quality Attributes (CQA)

Based on the scientific, therapeutic, industrial and regulatory aspects, QTPP for VPN loaded polymeric nanoparticles were established. Further, based on the prior knowledge, literature review and experiment trials, three response variables viz., particle size, drug entrapment and drug loading were selected as CQA.

6A.2.2.2 Identification of Independent variables (factors) and qualitative risk assessment

Ishikawa diagram was used to demonstrate all the probable variables associated with development of VPN loaded PNP by nanoprecipitation method. These factors were qualitatively categorized as 'low, medium and high risk' based on their impact on CQA as described in Table 6A-1.

Table 6A-1. Quality risk assessment criteria

Low Risk	Factors with wide range of acceptability. No investigation required
Medium Risk	Acceptable risk. No adverse effect on product quality on small changes.
High Risk	Unacceptable risk. Acceptable range need to be investigated

Factors with low and medium risk were controlled by assigning constant levels based on literatures and preliminary trials.

6A.2.2.3 Quantitative risk assessment: Screening design

Factors with high risk were screened using 2-level fractional factorial design to statistically identify the critical factors and use them in main design to determine the control ranges (design space). Screening design was also utilized to assign constant levels of other non-critical factors. Minitab® 17.1.0 was used to generate a randomized design matrix based on which experimental batches were prepared and evaluated for CQA. Software based Pareto charts were utilized to determine critical factors while the main effect charts were utilized to decide the optimum levels of non-critical factors. Methods used for estimation of CQA are as follows

6A.2.2.3.1 Particle size and size distribution

Nanoparticulate dispersions were diluted ten times with pre-filtered distilled water, transferred to disposable sizing cuvette and analyzed by dynamic light scattering (DLS) using Nano-ZS Zetasizer, Malvern Instruments Ltd., UK for particle size (PS) and poly-dispersity index (PDI). The instrument analyzes angular scattering of a laser beam during its passage through the dispersed nanoparticulate sample and use the Mie theory of light scattering to calculate the mean diameter of nanoparticles.

6A.2.2.3.2 Drug entrapment and drug loading

Samples from nanoparticulate dispersions (0.1 ml) were dissolved and suitably diluted in acetonitrile and analyzed using uv-visible spectrophotometric method as described earlier in chapter 3. Drug

entrapment (%) and drug loading (%) were then calculated using **Eq. 6A-1** and **Eq. 6A-2**.

$$\text{Drug entrapment}(\%) = \frac{\text{Entrapped drug (mg)}}{\text{Total drug taken (mg)}} \times 100 \qquad \textbf{Eq. 6A-1}$$

$$\text{Drug loading}(\%) = \frac{\text{Entrapped drug (mg)}}{\text{Total polymeric nanoparticles (mg)}} \times 100 \qquad \textbf{Eq. 6A-2}$$

6A.2.2.4 Formulation optimization by Box Behnken response surface design

Box-Behnken response surface design was applied to exhaustively investigate the relationship between critical factors and CQA with less number of experimental batches [4]. Minitab® 17.1.0 was used for generating the randomized design matrix and statistical evaluation of experimental data to achieve optimization solution and creating the design space. Suitability of model suggested by the software and identification of significant model terms were decided based on analysis of variance followed by F-test. Insignificant model terms were later removed to simplify the mathematical equations for calculation of CQA. The relationship between critical factors and CQA was explored using contour and 3-D response surface plots. Desirability criteria was defined based on QTPP and design space was created to obtain final optimized batch. Three batches were prepared with optimized composition for model verification.

6A.2.3 In-vitro characterization of optimized VPN PNP

6A.2.3.1 Shape and surface morphology

The VPN PNP (VPN loaded PNP with optimized composition) were evaluated for shape and surface characteristics using transmission electron microscopy. Dispersion was spread on a carbon-coated grid, excess solution was removed and the grid was dried under infrared lamp. It was negatively stained with 2% phosphotungstic acid (PTA) and again dried under Infrared lamp. Transmission electron microscope (CM 200, Philips, Netherlands) with operating voltage range of 20-200 kV was used

to visualize nanoparticles at suitable enlargement with an accelerating voltage of 20 kV.

6A.2.3.2 Zeta potential

VPN PNP dispersion was diluted ten times with pre-filtered distilled water, transferred to disposable folded capillary cells and analyzed for zeta potential (ZP) using Nano-ZS zetasizer. The instrument utilizes Smoluchowski equation that calculates zeta potential based on amount of doppler shift occur due to electrophoretic mobility of colloidal particles in response to the electric field applied to the dispersion.

6A.2.3.3 In-vitro drug release study

The *in-vitro* drug release from optimized VPN PNP was evaluated using a Franz-type diffusion cell with an effective surface area of 3.14 cm^2 and a receptor chamber volume of 15 ml. Pre-activated dialysis membrane (MWCO, 12 kD) was mounted, as a permeation barrier, between donor and receptor chambers of diffusion cell. The receptor chamber was filled with a mixture of ethanol and double distilled water (ratio 3:7) as a diffusion media and allowed to equilibrate for half an hour. The optimized batches containing 1 mg of drug were transferred to donor chambers of diffusion cells. The diffusion medium was continuously stirred using a magnetic stirrer. 1 mL sample was withdrawn from sampling arm of diffusion cell at each time point up to 24 hours and equal volume of fresh diffusion media was added to maintain total receptor volume. Quantitative estimation of drug was performed by HPLC at 280 nm detection wavelength as described earlier in chapter 3A. The kinetics of drug release was then evaluated by fitting the data in various mathematical models and comparing their regression coefficient (R^2) values [5].

6A.3. RESULTS & DISCUSSION

6A.3.1 Preparation and optimization of VPN loaded polymeric nanoparticles

6A.3.1.1 Establishing QTPP and CQA

Various QTPP elements and their targets were defined and presented with justification in Table 6A-2.

Table 6A-2. QTPP elements with justification for VPN loaded PNP

QTPP element		Target	Justification
Route of administration		Transdermal	Avoid first pass metabolism and achieve prolonged action
Dosage form		Polymeric nanoparticle	Better skin permeability and controlled drug release
Formulation quality attributes	Particle size#	Minimize (~100 nm)	To ensure better permeation and drug release
	Polydispersity Index	Minimize (< 0.3)	To ensure uniformity of size and related characteristics.
	Zeta potential	> ±30 mV	To ensure stability of the dispersion
	Surface characteristics	Spherical, smooth	To ensure better permeation
	Drug entrapment#	Maximize	To minimize drug wastage for cost-effectiveness
	Drug loading#	Maximize	For better drug release and less polymer exposure
	In vitro Drug release behavior	Prolonged for 24 hours	To ensure controlled drug release for desired duration
Ex vivo permeability		Better transdermal flux	To ensure PK/ PD comparable to marketed formulations
Stability		NLT 1 months	To ensure stability till incorporation in final dosage form
Safety		Non-toxic & Non-irritant to skin	To ensure safety of the final formulation
Pharmacokinetics		Similar or better than oral suspension	For bioequivalence requirement
Pharmacodynamics			To demonstrate therapeutic efficacy

Critical quality attributes

Particle size, drug entrapment and drug loading were identified as critical in governing the product quality and need to be within known limits to attain the pre-defined QTPP. Thus, these three characteristics were selected as CQA.

6A.3.1.2 Identification and qualitative assessment of Independent variables (factors)

All the probable variables associated with development of VPN loaded PNP by nanoprecipitation method were identified during the brainstorming sessions and categorized in to Material, Process, Equipment, Personnel and Environment. An ishikawa diagram illustrating the cause and effect relationship among identified variables and CQA was constructed (**Fig. 6A-1**).

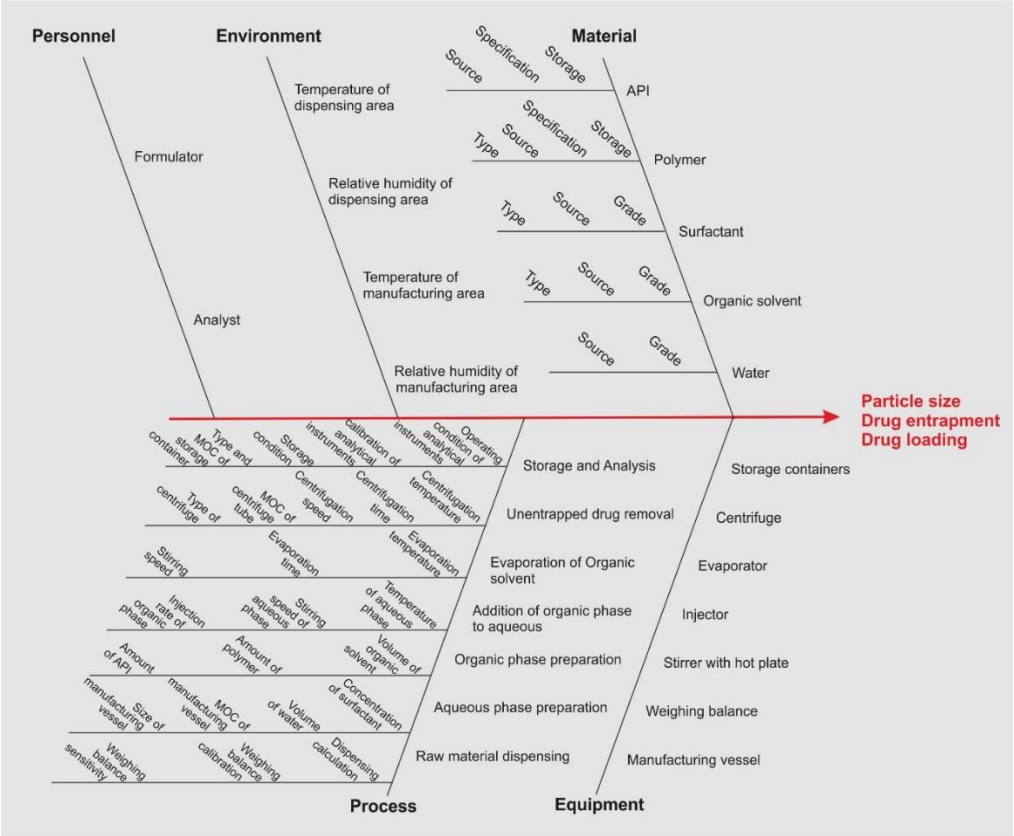

Fig. 6A-1. Ishikawa diagram showing probable variables that may influence the CQA

6A.3.1.3 Qualitative risk assessment

The risk associated with all the identified factors were evaluated based on the predefined criteria (**Table 6A-1**) and the result is presented in **Table 6A-3**. Factors with low and medium risk were assigned with the best available constant levels based on literature and preliminary trials to ensure no or negligible impact of these factors on CQA. These constant levels are also listed in **Table 6A-3**.

Table 6A-3. Qualitative risk assessment of independent variables

Factors	Process step	Impact on CQA	Constant levels
Source and specifications of API	Raw material Selection and Storage	Low risk	Authentic source with COA
Storage condition of API		Low risk	Stored at recommended condition
Type of Polymer		Low risk	PLGA 50:50
Source and specifications of Polymer		Low risk	Authentic source with COA
Storage condition of Polymer		Low risk	Stored at recommended condition
Type of Surfactant		Medium risk	Poloxamer 188
Source and specifications of Surfactant		Low risk	Authentic source
Storage condition of Surfactant		Low risk	Stored at recommended condition
Type of Organic solvent		Medium risk	Acetone
Source and specifications of Organic solvent		Low risk	Authentic source
Source of water		Low risk	In house
Grade of water		Low risk	Filtered (0.2µ) Double distilled
Weighing balance sensitivity	Dispensing	Low risk	0.1 mg
Weighing balance calibration		Low risk	Calibrated
Temperature and RH of Dispensing Area		Low risk	25±3°C, Ambient RH
Dispensing calculations		Low risk	Calculated using excel and verified
Type, Size and Material of Construction (MOC)	Manufacturing Vessel	Low risk	25 mL beaker of class A borosilicate glass
Temperature and Relative humidity	Manufacturing Area	Low risk	25±3°C, Ambient RH
Volume of Water	Aqueous phase preparation	Low risk	5 mL
Concentration of Surfactant		High risk	To be optimized
Amount of API	Organic phase preparation	High risk	To be optimized
Amount of Polymer		High risk	To be optimized
Volume of Organic solvent		High risk	To be optimized
Calibration of Injector and stirring equipment		Low risk	Calibrated

Factors	Process step	Impact on CQA	Constant levels
Injection Rate of Organic phase	Addition of Organic phase to aqueous	High risk	To be optimized
Stirring speed of Aqueous phase		High risk	To be optimized
Temperature of Aqueous phase		Low risk	Room temperature
Evaporation time	Evaporation of Organic solvent	Low risk	3-4 hours
Evaporation temperature		Low risk	Room temperature
Stirring speed during evaporation		Low risk	Same as used during organic phase addition
Type of Centrifuge	Unentrapped drug removal	Low risk	Cooling centrifuge
Type and MOC of Centrifuge tube		Low risk	15 mL conical-bottom glass tube with screw cap
Centrifugation speed		Medium risk	5000 rpm
Centrifugation time		Low risk	10 minutes
Centrifugation temperature		Low risk	15°C
Type and MOC of Storage container	Storage and Analysis	Low risk	20 mL flat-bottom glass vial with screw cap
Storage condition		Medium risk	2-8°C
Calibration of Analytical Instruments		Low risk	Calibrated
Methods used of Analysis		Low risk	Validated
Formulator	Personnel	Low risk	Common for all experiments and analysis
Analyst		Low risk	

Factors with high risk were carried forward for quantitative risk assessment.

6A.3.1.4 Quantitative risk assessment: Screening Design

Factors with high risk were statistically assessed by 2-level fractional factorial screening design. The low (-1) and high (+1) levels of all the independent variables were decided based on literatures as well as preliminary trials and are listed in **Table 6A-4**.

Table 6A-4. Various material attributes and process parameters along with their levels for screening by fractional factorial design

Independent variables		Unit	Levels	
			-1	+1
A:	Amount of Polymer (PLGA)	mg	20	40
B:	Amount of Drug	mg	1.0	2.0
C:	Surfactant concentration	% w/v	0.25	0.50
D:	Rate of polymer addition	mL/min	0.5	1.0
E:	Stirring speed	rpm	500	1000
F:	Volume of organic solvent	mL	2	4

The randomized design matrix of 17 experimental batches (including one center point) was generated using Minitab® 17.1.0 statistical software and presented in Table 6A-5.

Table 6A-5. Randomized batch matrix and resulting CQA for screening design

Batch no.	Run order	Independent Variables						CQA		
		A	B	C	D	E	F	Particle Size (nm)	Drug Entrapment (%)	Drug loading (%)
S_1	05	-1	-1	-1	-1	-1	-1	143.4	84.24	4.21
S_2	06	+1	-1	-1	-1	+1	-1	150.1	73.33	1.83
S_3	13	-1	+1	-1	-1	+1	+1	99.6	71.21	7.12
S_4	12	+1	+1	-1	-1	-1	+1	154.1	82.88	4.14
S_5	02	-1	-1	+1	-1	+1	+1	106.5	89.09	4.45
S_6	04	+1	-1	+1	-1	-1	+1	155.0	76.67	1.92
S_7	11	-1	+1	+1	-1	-1	-1	144.5	67.42	6.74
S_8	17	+1	+1	+1	-1	+1	-1	168.9	73.79	3.69
S_9	10	-1	-1	-1	+1	-1	+1	125.6	93.33	4.67
S_{10}	15	+1	-1	-1	+1	+1	+1	142.0	80.91	2.02
S_{11}	07	-1	+1	-1	+1	+1	-1	128.2	65.45	6.55
S_{12}	09	+1	+1	-1	+1	-1	-1	189.7	68.64	3.43
S_{13}	14	-1	-1	+1	+1	+1	-1	135.4	85.76	4.29
S_{14}	03	+1	-1	+1	+1	-1	-1	167.8	76.36	1.91
S_{15}	08	-1	+1	+1	+1	-1	+1	129.8	57.88	5.79
S_{16}	16	+1	+1	+1	+1	+1	+1	139.9	77.58	3.88
S_{17}	01	0	0	0	0	0	0	146.2	78.18	3.91

The data were statistically processed by Minitab software to generate pareto, normal and main effect plots for all three CQA considering $P < 0.05$ as a level of significance.

Pareto and normal charts (Fig. 6A-2) clearly showed that polymer amount, stirring speed and volume of organic solvent had a significant effect on particle size of resulting nanoparticles. Amount of polymer as well as drug showed significant impact on drug loading. Similarly, amount

of drug and its interactive effect with amount of polymer showed significant impact on drug entrapment. Owing to these observations, amount of polymer and amount of drug were selected as CMA while stirring speed and volume of organic solvent were selected as CPP for the final optimization step.

The influence of surfactant concentration and injection rate on the selected CQA was found insignificant. Hence, main effect plots were utilized to decide the constant level of these factors for final optimization step. Considering the positive impact on particle size and drug loading (**Fig. 6A-3**), lower levels of both the factors (surfactant concentration, 0.25 %w/v and injection rate, 0.5 mL/min) were chosen. Additionally, selecting lower surfactant concentration might improve product safety via less surfactant exposure.

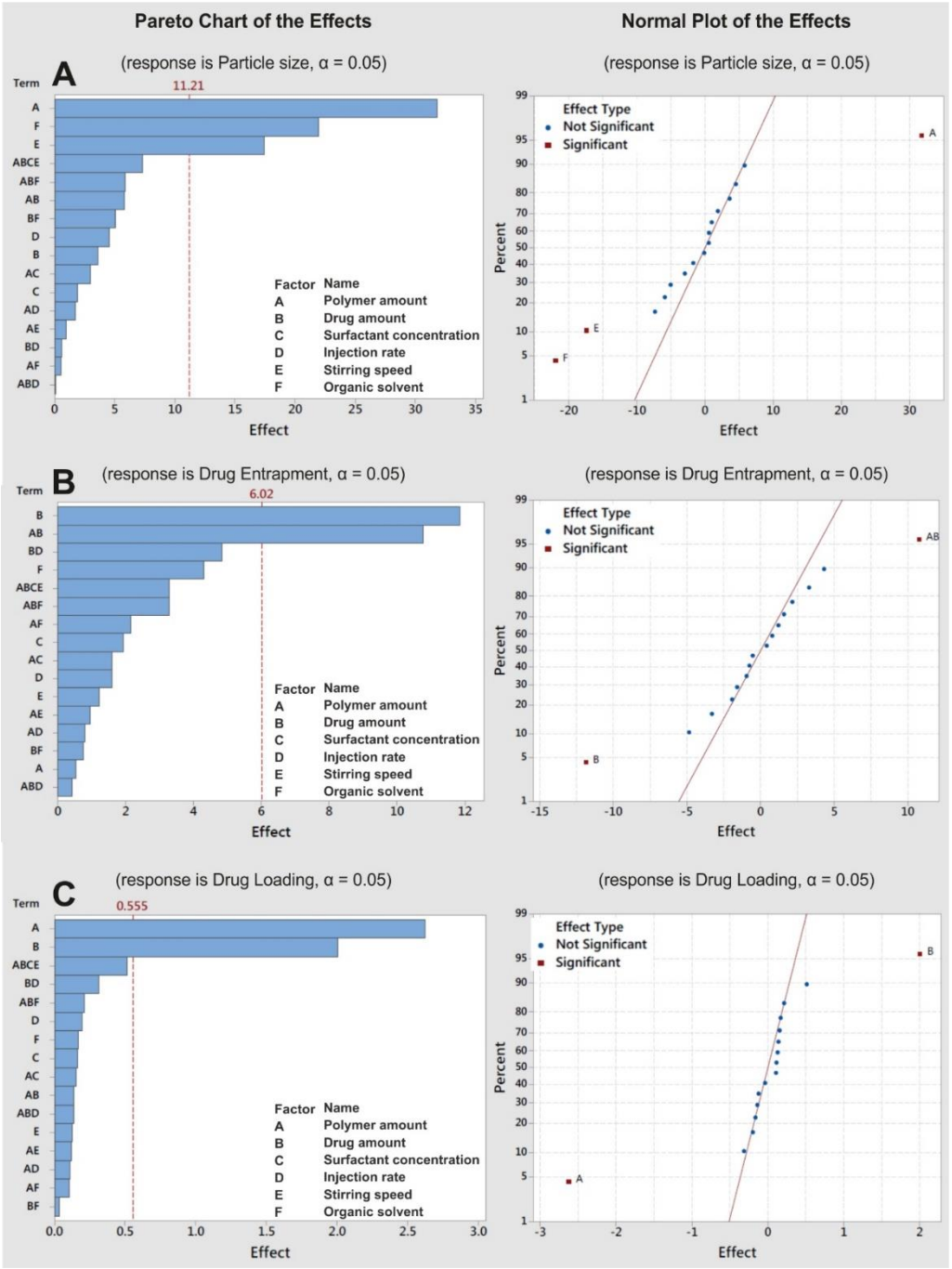

Fig. 6A-2. Pareto and Normal plots for A. Particle size, B. Drug entrapment and C. Drug loading

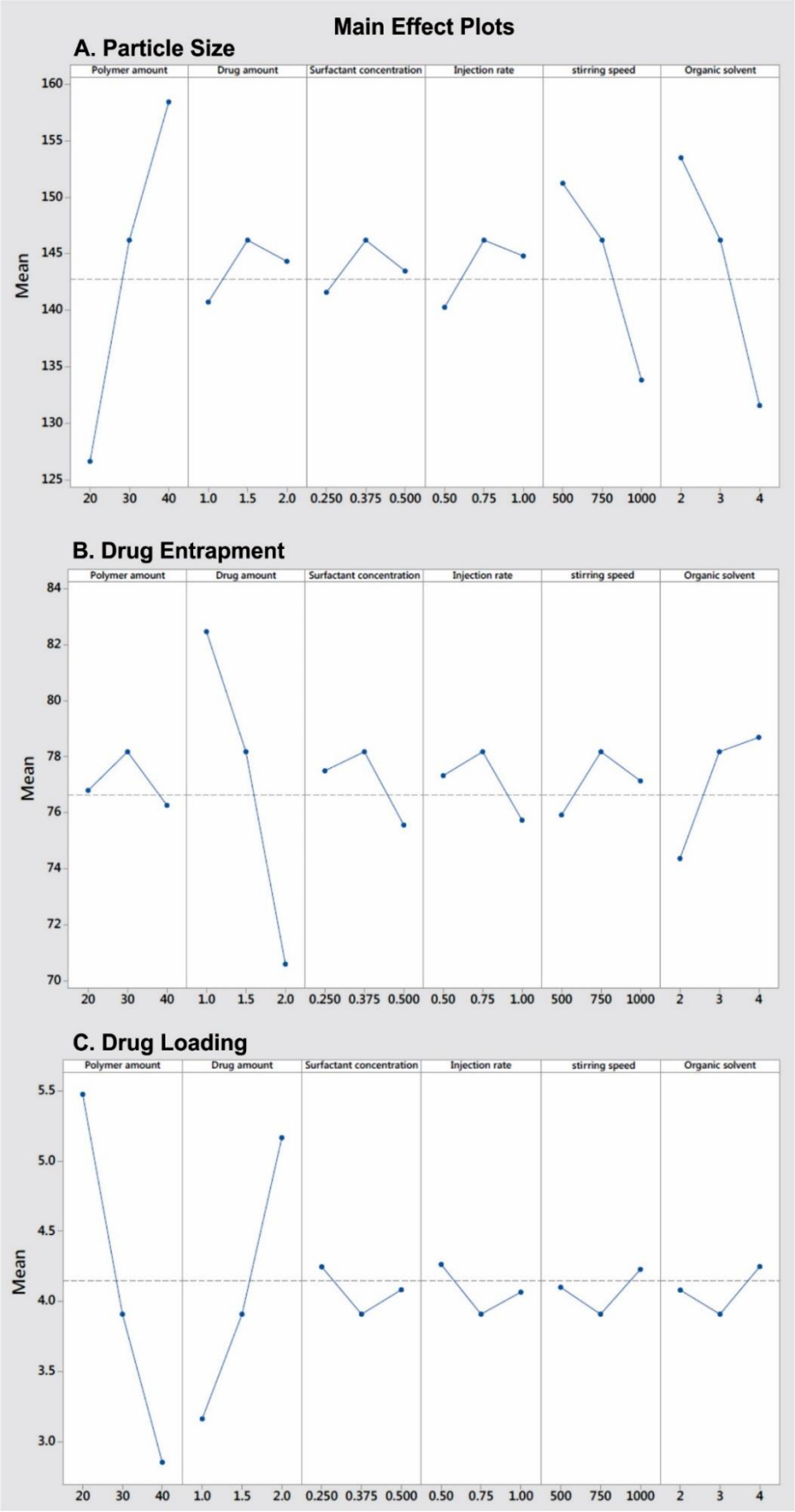

Fig. 6A-3. Main effect plots for A. Particle size, B. Drug entrapment and C. Drug loading

6A.3.1.5 Formulation optimization by Box Behnken response surface design

Based on the results of screening design, two CMA and two CPP were identified and their relationship with CQA were exhaustively investigated using Box-Behnken response surface design. Box-Behnken design was selected as it allows efficient estimation of quadratic terms with fewer design points that fall within safe operation limits as compared to central composite design [6]. The low (-1), medium (0) and high (+1) levels of all four CMA/CPP are listed in **Table 6A-6**.

Table 6A-6. Various critical material attributes and critical process parameters along with their levels for screening by Box-Behnken design

Independent variables (MAs/PPs)		Unit	Levels		
			-1	0	+1
A:	Amount of Polymer (PLGA)	mg	20	30	40
B:	Amount of Drug	mg	1.0	1.5	2.0
C:	Stirring speed	rpm	500	750	1000
D:	Volume of organic solvent	mL	2	3	4

A randomized matrix of twenty nine batches including five center points was generated by Minitab and presented in **Table 6A-7**. These batches were formulated as per their run order and evaluated for CQA using the methods described earlier. **Table 6A-7** also represents the resulting CQA of these batches.

Table 6A-7. Randomized design matrix for Box-Behnken response surface design

Batch no.	Run order	Independent Variables				CQA		
		A	B	C	D	Particle size (nm)	Drug entrapment (%)	Drug loading (%)
F_1	13	-1	-1	0	0	127.1	83.89	4.19
F_2	07	+1	-1	0	0	156.4	88.81	2.22
F_3	17	-1	+1	0	0	126.5	71.41	7.14
F_4	19	+1	+1	0	0	158.2	88.77	4.44
F_5	08	0	0	-1	-1	161.6	84.95	4.25
F_6	04	0	0	+1	-1	146.1	80.78	4.04
F_7	24	0	0	-1	+1	141.5	83.06	4.15
F_8	28	0	0	+1	+1	122.2	81.06	4.05
F_9	21	-1	0	0	-1	138.4	75.75	5.68
F_{10}	18	+1	0	0	-1	169.7	86.16	3.23
F_{11}	02	-1	0	0	+1	115.7	74.25	5.57
F_{12}	25	+1	0	0	+1	148.2	84.59	3.17
F_{13}	10	0	-1	-1	0	152.5	86.45	2.88

Batch no.	Run order	Independent Variables				CQA		
		A	B	C	D	Particle size (nm)	Drug entrapment (%)	Drug loading (%)
F_{14}	26	0	+1	-1	0	150.6	80.16	5.34
F_{15}	22	0	-1	+1	0	133.7	87.25	2.91
F_{16}	20	0	+1	+1	0	136.8	79.85	5.32
F_{17}	01	-1	0	-1	0	135.8	74.13	5.56
F_{18}	27	+1	0	-1	0	167.4	84.93	3.18
F_{19}	11	-1	0	+1	0	117.3	77.29	5.80
F_{20}	12	+1	0	+1	0	150.0	87.35	3.28
F_{21}	06	0	-1	0	-1	151.4	84.07	2.80
F_{22}	05	0	+1	0	-1	153.1	79.07	5.27
F_{23}	23	0	-1	0	+1	129.6	86.36	2.88
F_{24}	29	0	+1	0	+1	132.2	82.36	5.49
F_{25}	15	0	0	0	0	149.2	83.75	4.19
F_{26}	09	0	0	0	0	146.7	81.84	4.09
F_{27}	03	0	0	0	0	145.4	84.32	4.22
F_{28}	16	0	0	0	0	147.2	80.95	4.05
F_{29}	14	0	0	0	0	143.8	80.30	4.02

Analysis of variance (ANOVA) was performed by the software for full quadratic model consisting of Linear, quadratic and two-way interaction terms. Model terms with a p-value less than or equal to 0.05 (α-level) were considered as significant while terms with higher p-value were considered insignificant. Hierarchy based removal of insignificant model terms was done to simplify the model. ANOVA and coded coefficients of Full as well as reduced quadratic model for particle size are presented in Table 6A-8 and Table 6A-9, respectively.

Table 6A-8. Analysis of variance of full as well as reduced quadratic model for particle size

Source	Full model					Reduced model (α out - 0.1)*				
	DF	Adj SS	Adj MS	F-Value	P-Value	DF	Adj SS	Adj MS	F-Value	P-Value
Model	14	5378.94	384.21	204.58	0	7	23304	3329.1	136.14	0
Linear	4	5300.78	1325.2	705.64	0	4	22586.7	5646.7	230.9	0
A	1	2979.9	2979.9	1586.74	0	1	13743.1	13743.1	561.98	0
B	1	3.74	3.74	1.99	0.18	1	80.1	80.1	3.27	0.085
C	1	889.24	889.24	473.5	0	1	4989.8	4989.8	204.04	0
D	1	1427.9	1427.9	760.33	0	1	3773.7	3773.7	154.31	0
Square	4	65.99	16.5	8.78	0.001	3	717.3	239.1	9.78	0
A^2	1	25.32	25.32	13.48	0.003	1	238.8	238.8	9.76	0.005
B^2	1	34.34	34.34	18.28	0.001	1	348.3	348.3	14.24	0.001
C^2	1	12.28	12.28	6.54	0.023	1	354.4	354.4	14.49	0.001
D^2	1	28.63	28.63	15.24	0.002					
2-Way Interaction	6	12.17	2.03	1.08	0.42					
AB	1	1.44	1.44	0.77	0.396					
AC	1	0.3	0.3	0.16	0.694					

Source	Full model					Reduced model (α out - 0.1)*				
	DF	Adj SS	Adj MS	F-Value	P-Value	DF	Adj SS	Adj MS	F-Value	P-Value
AD	1	0.36	0.36	0.19	0.668					
BC	1	6.25	6.25	3.33	0.09					
BD	1	0.2	0.2	0.11	0.747					
CD	1	3.61	3.61	1.92	0.187					
Error	14	26.29	1.88			21	513.5	24.5		
Lack-of-Fit	10	9.98	1	0.24	0.968	17	473.6	27.9	2.79	0.166
Pure Error	4	16.31	4.08			4	40	10		
Total	28	5405.23				28	23817.5			

* Shaded rows represent insignificant model terms removed during model reduction

ANOVA table for particle size showed insignificant interaction effect among selected CMA/CPP. However, the quadratic and linear effects were found significant. Significant quadratic terms indicated that the relationship between these CMA/CPP and particle size follow a curved line. Amount of polymer, stirring speed and volume of organic solvent were found to significantly influence the particle size. An insignificant lack-of fit showed the adequacy of the model in explaining the variation in the responses.

Table 6A-9. Coded coefficients of full as well as reduced quadratic model for particle size

Term	Full Model					Reduced model (α out - 0.1)*				
	Effect	Coef	SE Coef	T-Value	VIF	Effect	Coef	SE Coef	T-Value	VIF
Constant		146.46	0.613	238.98			144.28	1.82	79.37	
A	31.517	15.758	0.396	39.83	1	67.68	33.84	1.43	23.71	1
B	1.117	0.558	0.396	1.41	1	5.17	2.58	1.43	1.81	1
C	-17.217	-8.608	0.396	-21.76	1	-40.78	-20.39	1.43	-14.28	1
D	-21.817	-10.908	0.396	-27.57	1	-35.47	-17.73	1.43	-12.42	1
A^2	-3.952	-1.976	0.538	-3.67	1.08	-11.92	-5.96	1.91	-3.12	1.05
B^2	-4.602	-2.301	0.538	-4.28	1.08	-14.39	-7.2	1.91	-3.77	1.05
C^2	-2.752	-1.376	0.538	-2.56	1.08	-14.52	-7.26	1.91	-3.81	1.05
D^2	-4.202	-2.101	0.538	-3.9	1.08					
AB	1.2	0.6	0.685	0.88	1					
AC	0.55	0.275	0.685	0.4	1					
AD	0.6	0.3	0.685	0.44	1					
BC	2.5	1.25	0.685	1.82	1					
BD	0.45	0.225	0.685	0.33	1					
CD	-1.9	-0.95	0.685	-1.39	1					

* Shaded rows represent insignificant model terms removed during model reduction

Coefficients table for particle size showed VIF values near to 1 indicating that the predictors are not correlated and regression coefficients are well estimated. Regression equations for full and reduced models in uncoded units are presented as **Eq. 6A-3** and **Eq. 6A-4**, respectively. The positive and negative sign before each coefficients indicates a direct or inverse relationship of that model term with particle size.

Full model

$$R1 = -101.6 + 2.409A + 16.28B - 0.0083C + 2.97D - 0.01976A^2 - 9.2B^2 - 0.000022C^2 - 2.101D^2 + 0.12AB + 0.00011AC + 0.03AD + 0.01BC + 0.45BD - 0.0038CD$$

Eq. 6A-3

Reduced model

$$R1 = -34.3 + 6.96A + 91.5B + 0.0926C - 17.73D - 0.0596A^2 - 28.78B^2 - 0.000116C^2$$

Eq. 6A-4

ANOVA and coded coefficients of Full as well as reduced quadratic model for drug entrapment are presented in **Table 6A-10** and **Table 6A-11**, respectively.

Table 6A-10. Analysis of variance of full as well as reduced quadratic model for drug entrapment

Source	Full model					Reduced model (α out - 0.1)*				
	DF	Adj SS	Adj MS	F-Value	P-Value	DF	Adj SS	Adj MS	F-Value	P-Value
Model	14	514.525	36.752	10.58	0	5	510.677	102.135	44.76	0
Linear	4	443.478	110.869	31.91	0	2	443.409	221.704	97.16	0
A	1	340.085	340.085	97.9	0	1	340.085	340.085	149.04	0
B	1	103.323	103.323	29.74	0	1	103.323	103.323	45.28	0
C	1	0.001	0.001	0	0.989					
D	1	0.069	0.069	0.02	0.89					
Square	4	30.456	7.614	2.19	0.123	2	28.554	14.277	6.26	0.007
A^2	1	8.546	8.546	2.46	0.139	1	8.081	8.081	3.54	0.073
B^2	1	14.433	14.433	4.15	0.061	1	16.742	16.742	7.34	0.013
C^2	1	0.056	0.056	0.02	0.901					
D^2	1	1.663	1.663	0.48	0.5					
2-Way Interaction	6	40.591	6.765	1.95	0.143	1	38.715	38.715	16.97	0
AB	1	38.715	38.715	11.14	0.005	1	38.715	38.715	16.97	0
AC	1	0.137	0.137	0.04	0.845					
AD	1	0.001	0.001	0	0.985					
BC	1	0.311	0.311	0.09	0.769					
BD	1	0.254	0.254	0.07	0.791					
CD	1	1.173	1.173	0.34	0.57					
Error	14	48.635	3.474			23	52.483	2.282		
Lack-of-Fit	10	36.441	3.644	1.2	0.468	19	40.289	2.12	0.7	0.74
Pure Error	4	12.194	3.048			4	12.194	3.048		
Total	28	563.16				28	563.16			

* Shaded rows represent insignificant model terms removed during model reduction

ANOVA table for drug entrapment showed significant interaction, quadratic and linear effects among selected CMA/CPP. Observing the individual terms showed that amount of polymer and amount of drug had significant interaction, quadratic and linear effect on drug entrapment. Significant quadratic terms indicated that the relationship between these CMA and particle size follow a curved line. An insignificant

lack-of fit showed the adequacy of the model in explaining the variation in the responses.

Table 6A-11. Coded coefficients of full as well as reduced quadratic model for drug entrapment

Term	Full Model					Reduced model (α out - 0.1)*				
	Effect	Coef	SE Coef	T-Value	VIF	Effect	Coef	SE Coef	T-Value	VIF
Constant		82.232	0.834	98.65			82.006	0.455	180.05	
A	10.647	5.324	0.538	9.89	1	10.647	5.324	0.436	12.21	1
B	-5.869	-2.934	0.538	-5.45	1	-5.869	-2.934	0.436	-6.73	1
C	-0.015	-0.008	0.538	-0.01	1					
D	0.151	0.076	0.538	0.14	1					
A^2	-2.296	-1.148	0.732	-1.57	1.08	-2.164	-1.082	0.575	-1.88	1.02
B^2	2.983	1.492	0.732	2.04	1.08	3.115	1.557	0.575	2.71	1.02
C^2	0.185	0.093	0.732	0.13	1.08					
D^2	-1.013	-0.506	0.732	-0.69	1.08					
AB	6.222	3.111	0.932	3.34	1	6.222	3.111	0.755	4.12	1
AC	-0.37	-0.185	0.932	-0.2	1					
AD	-0.036	-0.018	0.932	-0.02	1					
BC	-0.558	-0.279	0.932	-0.3	1					
BD	0.504	0.252	0.932	0.27	1					
CD	1.083	0.542	0.932	0.58	1					

* Shaded rows represent insignificant model terms removed during model reduction

Coefficients table for drug entrapment showed VIF values near to 1 indicating that the predictors are not correlated and regression coefficients are well estimated. Regression equations for full and reduced models in uncoded units are presented as **Eq. 6A-5** and **Eq. 6A-6**, respectively. The positive and negative sign before each coefficients indicates a direct or inverse relationship of that model term with drug entrapment.

Full model

$$R2 = 105.0 + 0.349A - 42.3B - 0.0032C + 0.79D - 0.01148A^2 + 5.97B^2 + 0.000001C^2 - 0.506D^2 + 0.622AB - 0.000074AC - 0.0018AD - 0.00223BC + 0.50BD + 0.00217CD$$

Eq. 6A-5

Reduced model

$$R2 = 107.1 + 0.248A - 43.22B - 0.01082A^2 + 6.23B^2 + 0.622AB$$ **Eq. 6A-6**

ANOVA and coded coefficients of Full as well as reduced quadratic model for drug loading are presented in **Table 6A-12** and **Table 6A-13**, respectively.

Table 6A-12. Analysis of variance of full as well as reduced quadratic model for drug loading

Source	Full model					Reduced model (α out - 0.1)*				
	DF	Adj SS	Adj MS	F-Value	P-Value	DF	Adj SS	Adj MS	F-Value	P-Value
Model	14	37.3553	2.6682	270.23	0	4	37.3344	9.3336	1407.74	0
Linear	4	36.3859	9.0965	921.26	0	2	36.3857	18.1928	2743.93	0
A	1	17.3276	17.3276	1754.88	0	1	17.3276	17.3276	2613.42	0
B	1	19.0581	19.0581	1930.15	0	1	19.0581	19.0581	2874.43	0
C	1	0.0001	0.0001	0.01	0.942					
D	1	0.0002	0.0002	0.02	0.899					
Square	4	0.8221	0.2055	20.82	0	1	0.8162	0.8162	123.1	0
A^2	1	0.7566	0.7566	76.63	0	1	0.8162	0.8162	123.1	0
B^2	1	0.0027	0.0027	0.27	0.611					
C^2	1	0.0001	0.0001	0.01	0.914					
D^2	1	0.0021	0.0021	0.21	0.653					
2-Way Interaction	6	0.1472	0.0245	2.49	0.075	1	0.1325	0.1325	19.99	0
AB	1	0.1325	0.1325	13.42	0.003	1	0.1325	0.1325	19.99	0
AC	1	0.0054	0.0054	0.54	0.473					
AD	1	0.0007	0.0007	0.07	0.792					
BC	1	0.0006	0.0006	0.06	0.814					
BD	1	0.0051	0.0051	0.52	0.482					
CD	1	0.0029	0.0029	0.3	0.594					
Error	14	0.1382	0.0099			24	0.1591	0.0066		
Lack-of-Fit	10	0.1078	0.0108	1.41	0.395	20	0.1286	0.0064	0.84	0.652
Pure Error	4	0.0305	0.0076			4	0.0305	0.0076		
Total	28	37.4935				28	37.4935			

* Shaded rows represent insignificant model terms removed during model reduction

ANOVA table for drug loading showed significant quadratic and linear effects but interaction effect was found insignificant. Observing the individual terms showed that interactive as well as linear effect of polymer and drug amount and quadratic effect of polymer amount was significant for drug loading. Significant quadratic terms indicated that the relationship between polymer amount and drug loading follow a curved line. An insignificant lack-of fit showed the adequacy of the model in explaining the variation in the responses.

Table 6A-13. Coded coefficients of full as well as reduced quadratic model for drug loading

Term	Full Model					Reduced model (α out - 0.1)*				
	Effect	Coef	SE Coef	T-Value	VIF	Effect	Coef	SE Coef	T-Value	VIF
Constant		4.1116	0.0444	92.52			4.1147	0.0197	208.35	
A	-2.4033	-1.2017	0.0287	-41.89	1	-2.4033	-1.2017	0.0235	-51.12	1
B	2.5205	1.2602	0.0287	43.93	1	2.5205	1.2602	0.0235	53.61	1
C	0.0043	0.0021	0.0287	0.07	1					
D	0.0074	0.0037	0.0287	0.13	1					
A^2	0.6831	0.3415	0.039	8.75	1.08	0.6812	0.3406	0.0307	11.1	1
B^2	0.0405	0.0203	0.039	0.52	1.08					
C^2	0.0086	0.0043	0.039	0.11	1.08					
D^2	-0.0359	-0.0179	0.039	-0.46	1.08					
AB	-0.3641	-0.182	0.0497	-3.66	1	-0.3641	-0.182	0.0407	-4.47	1

Term	Full Model					Reduced model (α out - 0.1)*				
	Effect	Coef	SE Coef	T-Value	VIF	Effect	Coef	SE Coef	T-Value	VIF
AC	-0.0732	-0.0366	0.0497	-0.74	1					
AD	0.0267	0.0133	0.0497	0.27	1					
BC	-0.0238	-0.0119	0.0497	-0.24	1					
BD	0.0717	0.0359	0.0497	0.72	1					
CD	0.0542	0.0271	0.0497	0.54	1					

* Shaded rows represent insignificant model terms removed during model reduction

Coefficients table for drug loading showed VIF values near to 1 indicating that the predictors are not correlated and regression coefficients are well estimated. Regression equations for full and reduced models in uncoded units are presented as **Eq. 6A.7** and **Eq. 6A.8**, respectively. The positive and negative sign before each coefficients indicates a direct or inverse relationship of that model term with drug entrapment.

Full model

$$R3 = 5.66 - 0.2635A + 3.226B + 0.00016C - 0.118D + 0.003415A^2 + 0.081B^2 + 0.000000C^2 - 0.0179D^2 - 0.03641AB - 0.000015AC + 0.00133AD - 0.000095BC + 0.0717BD + 0.000108CD$$

Eq. 6A-7

Reduced model

$$R3 = 5.366 - 0.2699A + 3.613B + 0.003406A^2 - 0.03641AB$$ **Eq. 6A-8**

Model summary for all the three CQA is presented in **Table 6A-14**. A low S value and high R^2 value indicated a better prediction of responses by the model. Predicted R^2 was found to be in good agreement with other R^2 further supporting the prediction potential of the model.

Table 6A-14. Summary of full as well as reduced quadratic model for all three CQA

Responses	Full model				Reduced model (α out - 0.1)			
	S	R-sq	R-sq (adj)	R-sq (pred)	S	R-sq	R-sq (adj)	R-sq (pred)
Particle size (nm)	1.3704	99.51	99.03	98.46	4.94517	97.84	97.13	95.65
Drug entrapment (%)	1.86385	91.36	82.73	59.34	1.51058	90.68	88.65	85.58
Drug loading (%)	0.099368	99.63	99.26	98.22	0.081426	99.58	99.50	99.34

Four different residual plots viz., normal probability plot, residual versus fitted values, histogram and residual versus order of data were generated for all three CQA and presented in **Fig. 6A-4**. In normal probability graph, residuals were appeared to follow a straight line indicating that the data was normally distributed. Residual versus fitted values graph and residual versus order of data graph showed random

scattering of residuals around zero indicating a constant variance and uncorrelated error, respectively.

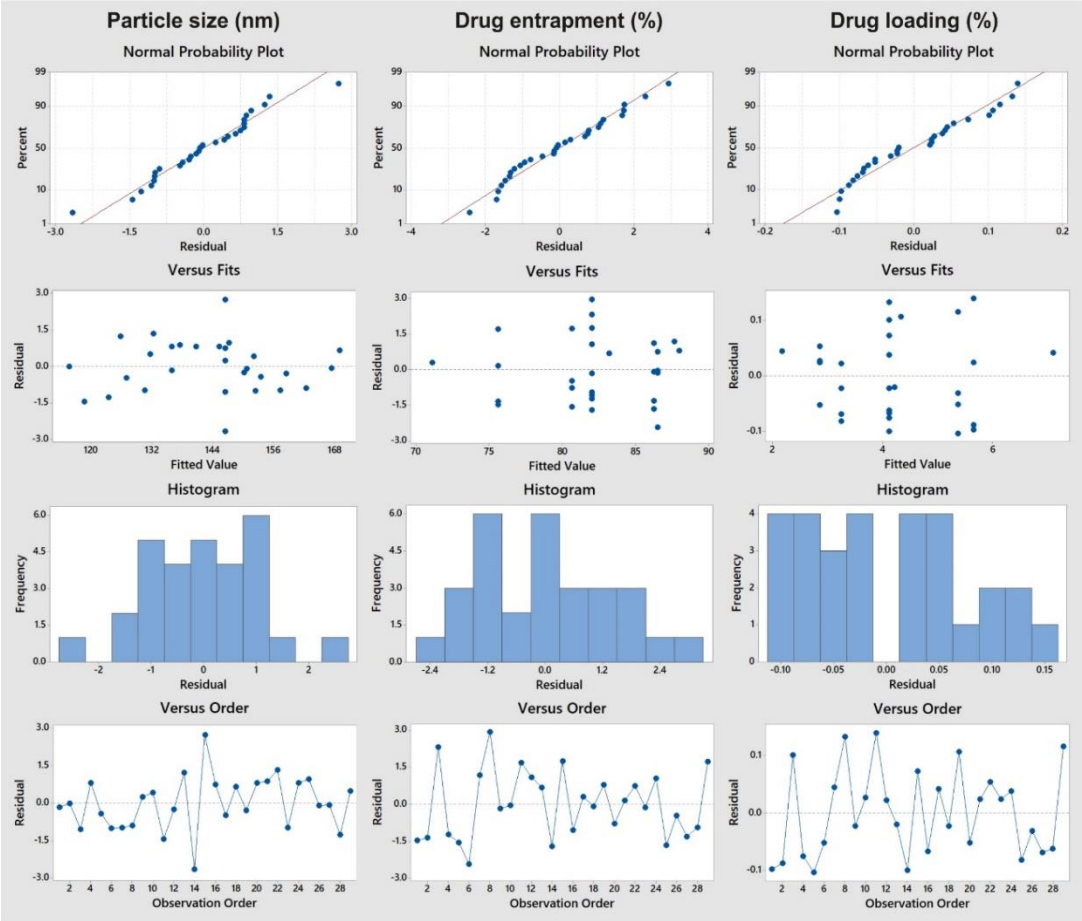

Fig. 6A-4. Residual plots for all three CQA

The main effect plots for all three CQA are presented in **Fig. 6A-5**. These graphs provided a better depiction of how the individual CMA/CPP influence respective CQA and found in-line with the ANOVA results.

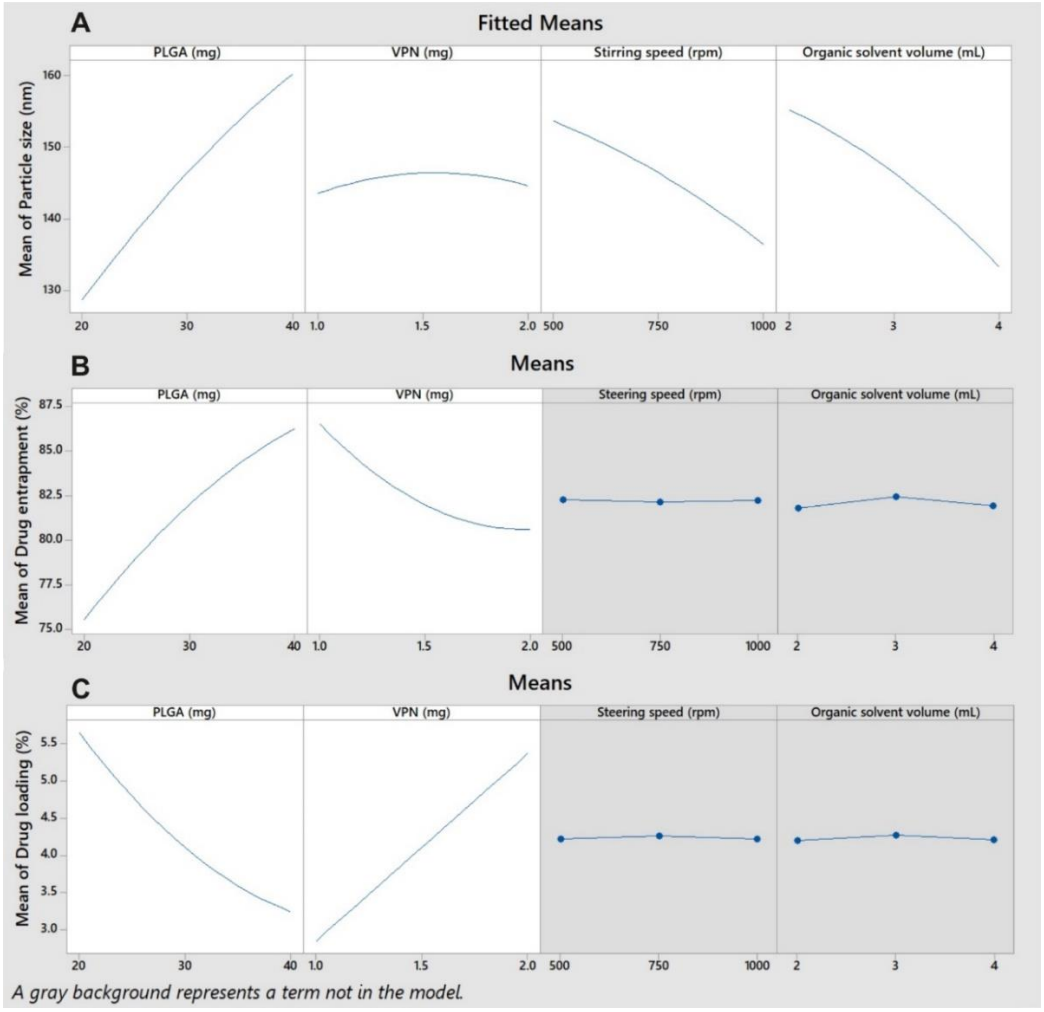

Fig. 6A- 5. Main effect plots of reduced quadratic model for A. particle size, B. drug entrapment and C. drug loading

Contour and response surface plots are presented in **Fig. 6A-6** and **Fig. 6A-7**, respectively. These graphs were used to depict how the CQA is related to any two CMA/CPP while keeping other CMA/CPP at constant levels.

Overlaid contour plots for all three CQA were generated for their desirable range (**Fig. 6A-8**) to observe the design space (white area in graph). The overlaid plot between PLGA and VPN at 1000 rpm stirring speed and 4 mL organic solvent volume, showed a design space with largest area at lower PLGA and higher VPN amount. Further, the response optimizer plot was generated using the criteria shown in **Table 6A-15**. The target for drug entrapment was set at 70% to maximize the drug loading which was desirable for better drug release and to reduce polymer exposure.

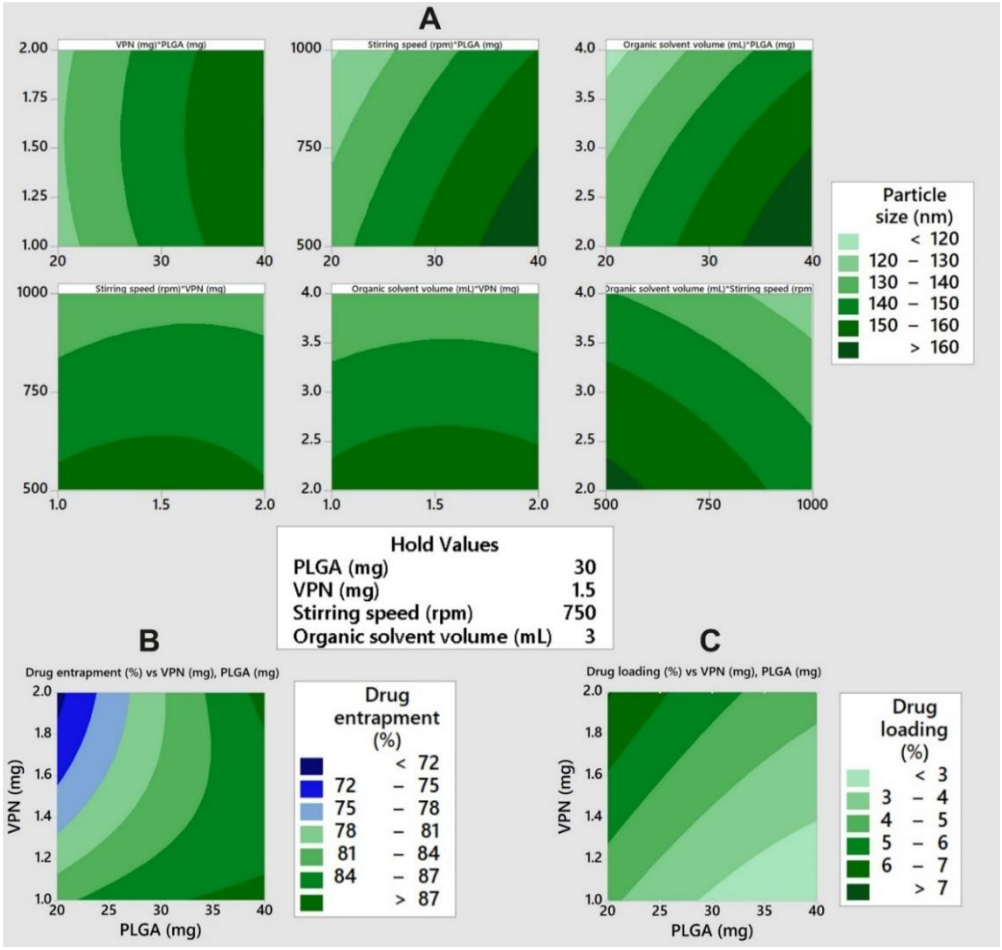

Fig. 6A-6. Contour plots of reduced quadratic model for A. particle size, B. drug entrapment and C. drug loading

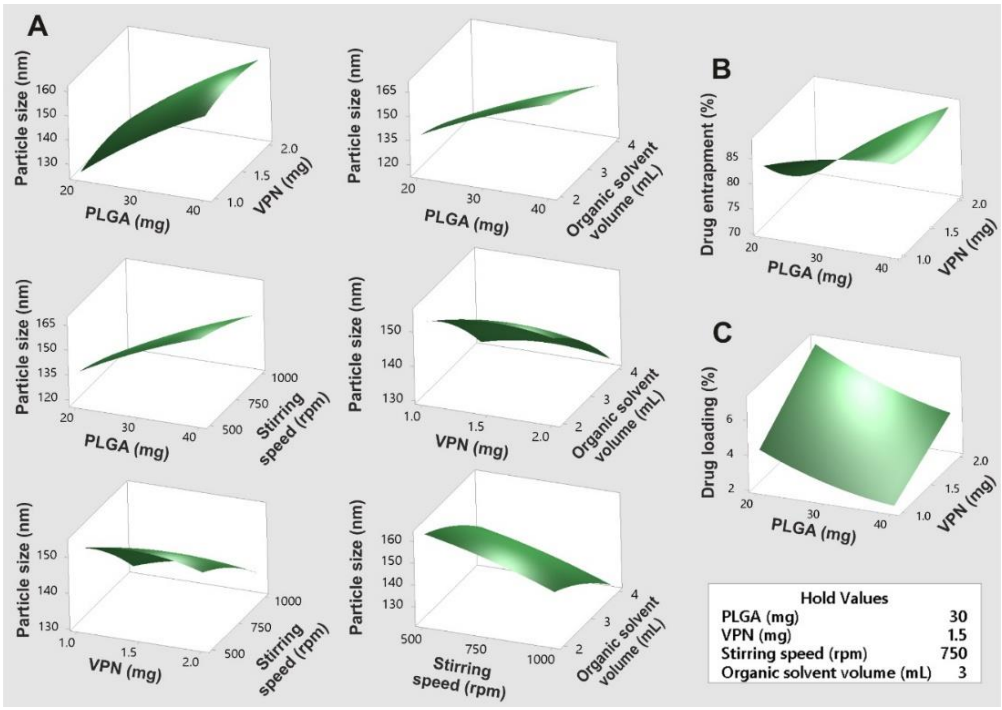

Fig. 6A-7. Response surface plots of reduced quadratic model for A. particle size, B. drug entrapment and C. drug loading

Table 6A-15. Criteria for optimization of VPN PNP

Responses	Goal	Lower	Target	Upper	Weight	Importance
Particle size (nm)	Minimum	115.7	-	169.7	1	1
Drug entrapment (%)	Target	63	70	88.806	1	1
Drug loading (%)	Maximum	2.2201	-	7.1409	1	1

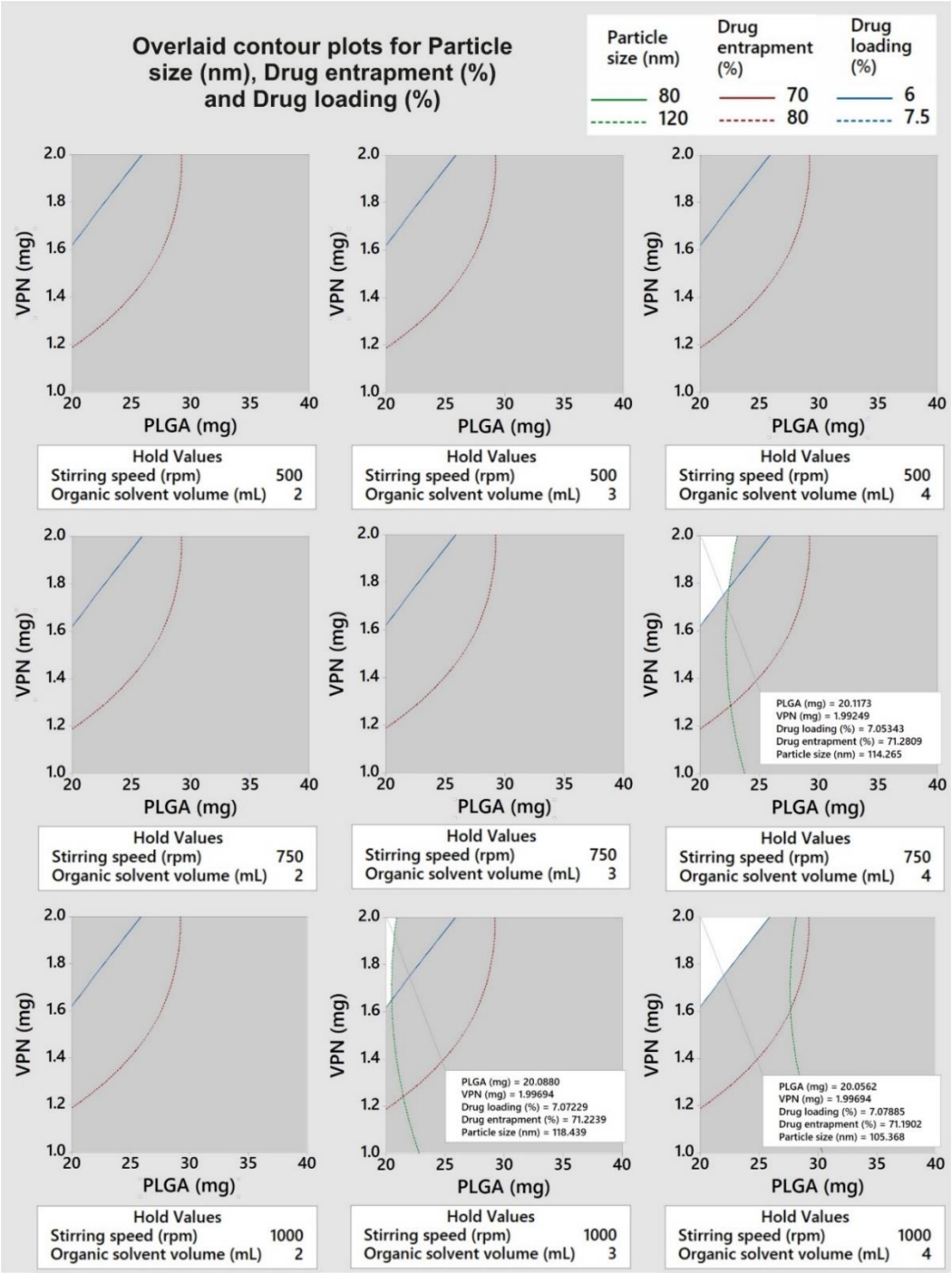

Fig. 6A-8. Overlaid contour plots of reduced quadratic model with higher and lower range of all three CQA showing design space

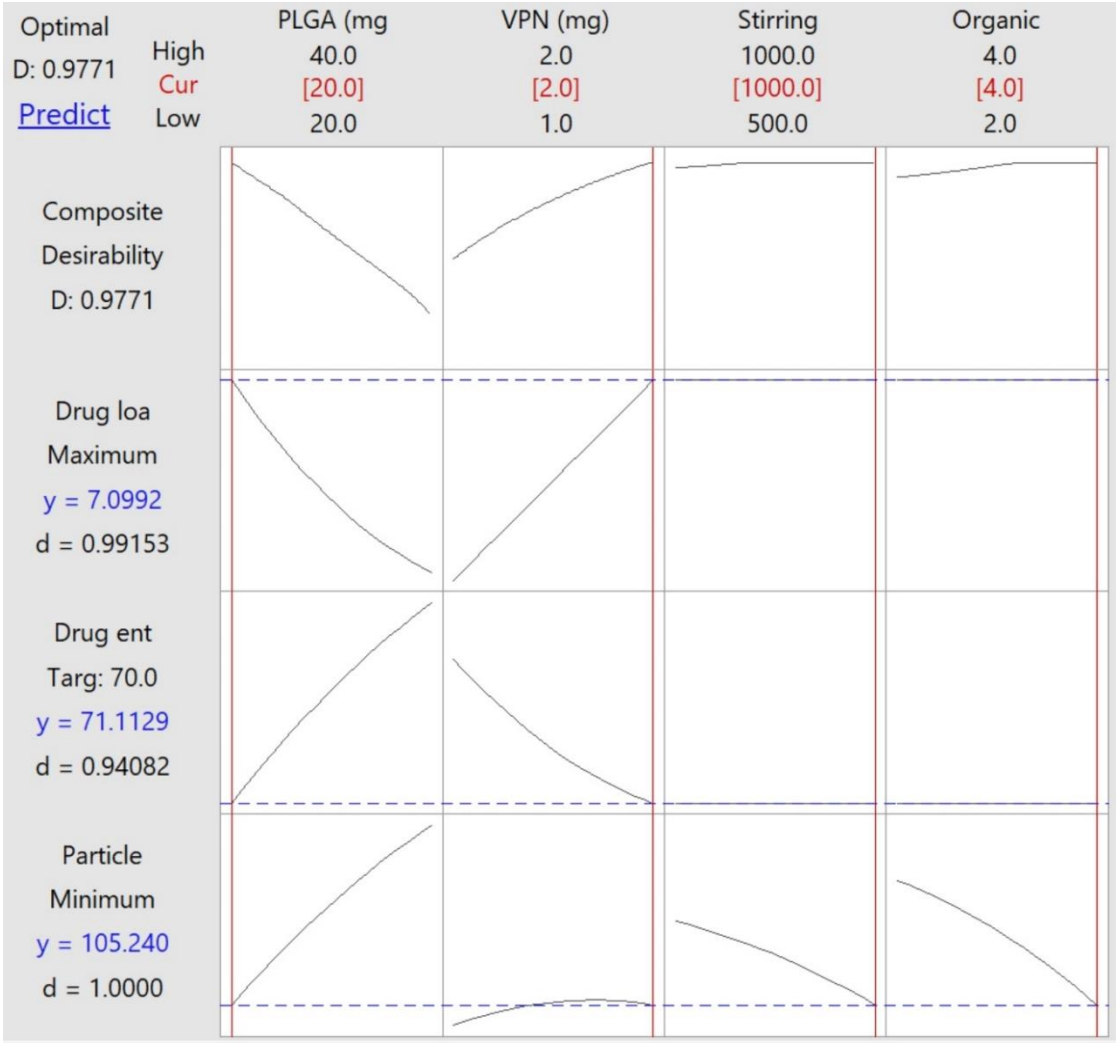

Fig. 6A-9. Response optimizer plot showing individual and composite desirability of predicted optimum levels

The response optimizer plot (**Fig. 6A-9**) showed an optimization solution having a composite desirability of 0.9771. the setting of this optimization solution is also presented in **Table 6A-16** along with the 95% confidence as well as 95% prediction intervals. Three batches with optimized levels were prepared for verification trials and the values of different CQA are presented in **Table 6A-17**.

The average values of all three CQA were found to fall within 95% confidence interval and thus indicated the validity of the model.

Table 6A-16. Optimization solution

Multiple Response Prediction

Variable	Setting
PLGA (mg)	20
VPN (mg)	2
Stirring speed (rpm)	1000
Organic solvent volume (mL)	4

Responses	Fit	SE Fit	95% Confidence interval		95% Prediction interval	
			Lower	Upper	Lower	Upper
Particle size (nm)	105.24	1.27	102.58	107.9	101.43	109.05
Drug entrapment (%)	71.11	1.13	68.77	73.46	67.2	75.02
Drug loading (%)	7.0992	0.0576	6.9804	7.2181	6.8934	7.3051

Table 6A-17. Results of verification trials

Responses	95% Prediction interval		Results			
	Lower	Upper	Batch-1	Batch-2	Batch-3	Average
Particle size (nm)	101.43	109.05	103.92	106.65	103.44	104.67
Drug entrapment (%)	67.2	75.02	69.91	72.73	72.14	71.59
Drug loading (%)	6.8934	7.3051	7.17	7.13	7.08	7.13

6A.3.2 In-vitro characterization of optimized VPN-PNP

6A.3.2.1 Shape and surface morphology

Transmission electron microscopy of optimized VPN-PNP was performed and the image is represented as **Fig. 6A-10**. The image showed spherical shape with smooth surface of nanoparticles. The size of nanoparticles seen in the image was found in-line with the results of particle size data obtained from Malvern zetasizer (**Fig. 6A-11**).

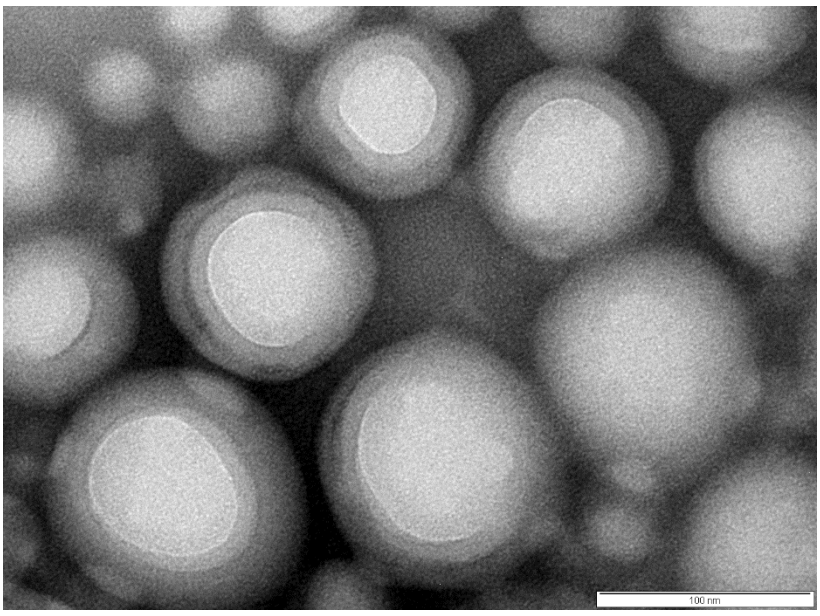

Fig. 6A-10. Transmission electron microscopic image of optimized VPN PNP

System

Temperature (°C):	25.1	**Duration Used (s):**	70
Count Rate (kcps):	176.2	**Measurement Position (mm):**	4.65
Cell Description:	Disposable sizing cuvette	**Attenuator:**	6

Results

			Size (r.nm):	% Intensity	Width (r.nm):
Z-Average (r.nm):	103.92	**Peak 1:**	104.30	100.0	27.96
PdI:	0.034	**Peak 2:**	0.000	0.0	0.000
Intercept:	0.947	**Peak 3:**	0.000	0.0	0.000

Result quality : Good

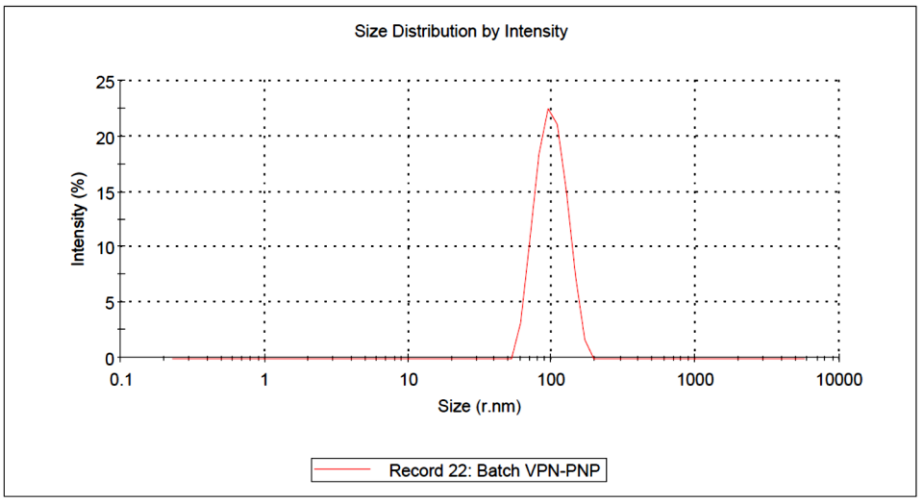

Fig. 6A-11. Size distribution graph of optimized VPN PNP

System

Temperature (°C):	25.0	**Zeta Runs:**	12
Count Rate (kcps):	185.3	**Measurement Position (mm):**	2.00
Cell Description:	Clear disposable zeta cell	**Attenuator:**	10

Results

			Mean (mV)	Area (%)	Width (mV)
Zeta Potential (mV):	-38.5	**Peak 1:**	-38.5	100.0	10.1
Zeta Deviation (mV):	10.1	**Peak 2:**	0.00	0.0	0.00
Conductivity (mS/cm):	0.0498	**Peak 3:**	0.00	0.0	0.00

Result quality : Good

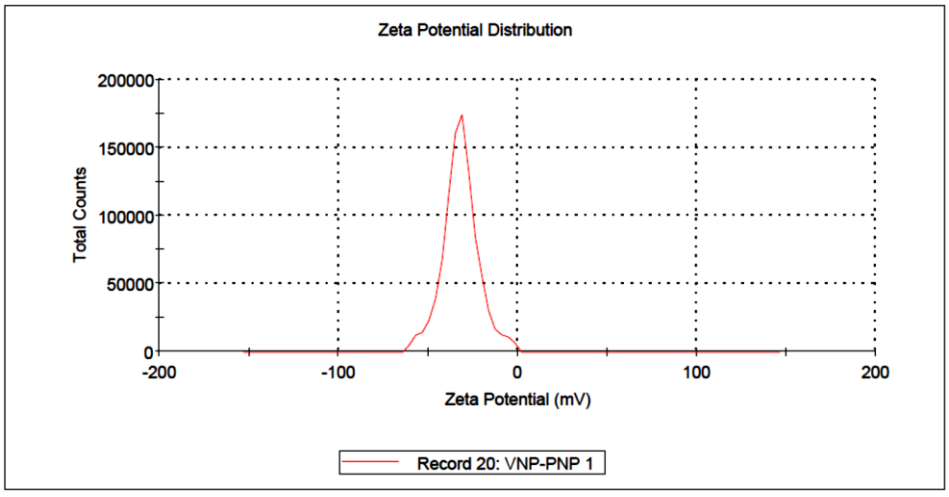

Fig. 6A-12. Zeta potential graph of optimized VPN PNP

6A.3.2.2 Zeta potential

The zeta potential graph of optimized VPN-PNP (**Fig. 6A-12**) showed a net negative charge on nanoparticle surface with a zeta potential value of -38.5 mV. The charge was found sufficient enough to keep the particles dispersed via repulsive forces [7, 8].

6A.3.2.3 In-vitro drug release study

In vitro drug release from VPN PNP was evaluated and the cumulative percent drug release at different time points are summarized in **Table 6A-18** as well as illustrated in **Fig. 6A-13**. In order to ensure that the presence of VPN in release media directly reflects its release from nanocarriers, the permeation of released VPN across dialysis membrane should not be rate limiting. Hence, data for VPN solution was also generated which showed >90% drug release within 2 hours indicating non-barrier nature of dialysis membrane for dissolved VPN. Release data of VPN PNP showed >50 % VPN release in first 8 hours and > 80 % release in 24 hours indicating the control release behavior of PNP.

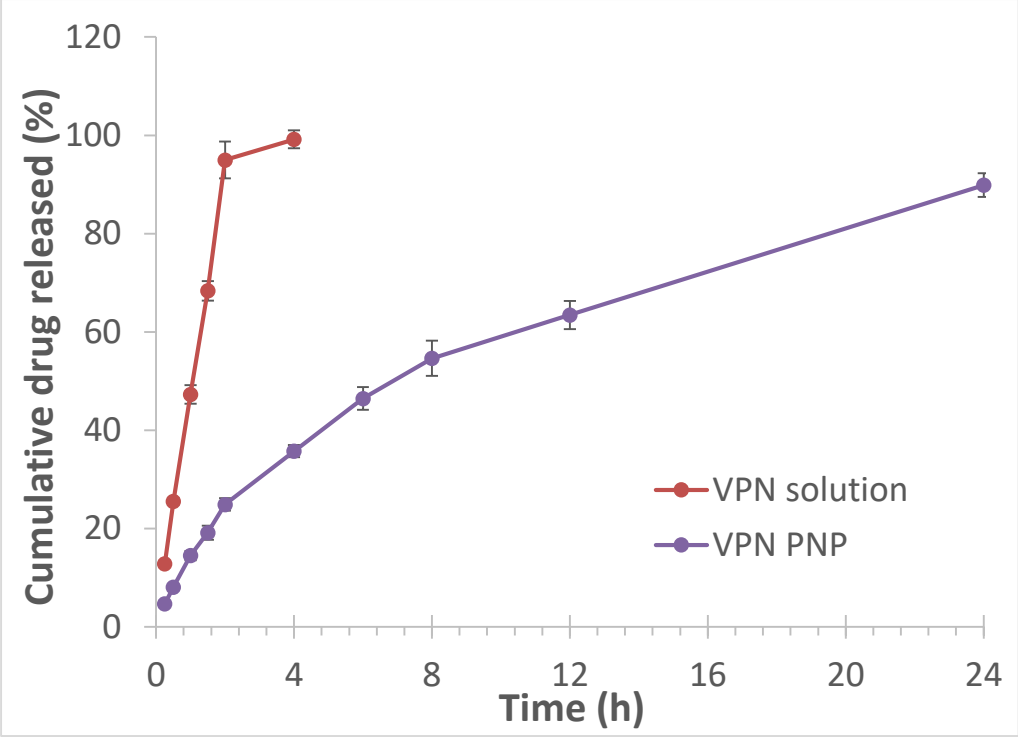

Fig. 6A-13. Cumulative percent of VPN released in vitro versus time curve for PNP

Table 6A-18. In vitro release profile of VPN from its solution and PNP

Time (h)	Cumulative percent drug released	
	VPN Solution*	VPN PNP*
0.25	12.78 ± 0.35	04.64 ± 0.27
0.5	25.54 ± 0.69	08.07 ± 0.34
1	47.27 ± 1.89	14.49 ± 0.93
1.5	68.35 ± 2.01	19.14 ± 1.43
2	94.97 ± 3.76	24.89 ± 1.28
4	99.16 ± 1.82	35.72 ± 1.24
6	-	46.45 ± 2.32
8	-	54.63 ± 3.56
12	-	63.43 ± 2.86
24	-	89.87 ± 2.44

* Result represented as mean ± SD

The result of various mathematical models, applied to understand the VPN release kinetics from PNP, are presented in Table 6A-19.

Table 6A-19. Various mathematical models and their correlation coefficient values

Mathematical models	Graph description (Y-axis versus X-axis)	VPN PNP	
		R^2	n
Zero order	Cumulative amount/percent of drug released *versus* time	0.951	-
First order	Log cumulative percent drug remaining *versus* time	-0.997	-
Higuchi	Cumulative percent drug released *versus* square root of time	0.998	-
Hixon Crowell	Cube root of percent drug remaining *versus* time	-0.994	-
Korsmeyer Peppas	Log cumulative percent drug released *versus* log time	0.993	0.68

The R^2 values for Higuchi as well as first order model was found higher suggesting a diffusion controlled system where release rate is dependent on remaining drug concentration within the carrier.

REFERENCES

1. Santander-Ortega, M., et al., *Nanoparticles made from novel starch derivatives for transdermal drug delivery.* Journal of controlled release, 2010. **141**(1): p. 85-92.
2. Barichello, J.M., et al., *Encapsulation of hydrophilic and lipophilic drugs in PLGA nanoparticles by the nanoprecipitation method.* Drug development and industrial pharmacy, 1999. **25**(4): p. 471-476.
3. Lawrence, X.Y., *Pharmaceutical quality by design: product and process development, understanding, and control.* Pharmaceutical research, 2008. **25**(4): p. 781-791.

4. Eriksson, L., et al., *Design of experiments.* Principles and Applications, Learn ways AB, Stockholm, 2000.
5. Quinn, H.L., et al., *Design of a Dissolving Microneedle Platform for Transdermal Delivery of a Fixed-Dose Combination of Cardiovascular Drugs.* J Pharm Sci, 2015. **104**(10): p. 3490-500.
6. *Minitab StatGuide, Minitab 17 Statistical Software*. 2010, Minitab, Inc.: State College, PA.
7. Salopek, B., D. Krasic, and S. Filipovic, *Measurement and application of zeta-potential.* Rudarsko-geolosko-naftni zbornik, 1992. **4**(1): p. 147.
8. *Zeta potential: An introduction in 30 minutes*. Zetasizer Nano series technical note 2017 [cited 2017; Available from: https://www.materials-talks.com/wp-content/uploads/2017/09/mrk654-01_an_introduction_to_zeta_potential_v3.pdf.

Chapter 6B

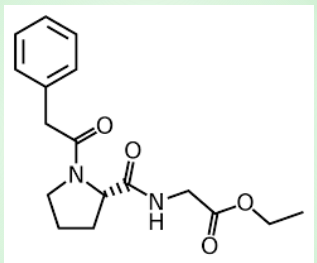

Formulation Development

Polymeric Nanoparticles

Noopept

Contents

6B.1. INTRODUCTION

With an objective to achieve therapeutic plasma levels of NPT via transdermal route, polymeric nanoparticles (PNP) were also developed. Ability of these nanocarriers to flow through the narrow intercellular pores and carry the payload to deeper skin layers have been widely reported in literatures [1]. Out of several available methods for preparation, the nanoprecipitation method was used [2]. A systematic quality-by-design (QbD) approach employing statistical design of experiments was utilized for optimization via establishing the impact of material attributes and process parameters on the critical formulation attributes [3].

6B.2. MATERIALS & METHODS

6B.2.1 Materials

Noopept (NPT) was purchased from Nootrico S.A., US. PLGA 50:50 was kindly gifted by Purac Biomaterials, Netherlands. Poloxamer 188 was received from BASF, Ludwigshafen, Germany as gift sample. Dialysis bags (MWCO, 12 kD) were purchased from HiMedia Labs Pvt.

Ltd., Mumbai, India. Double distilled water was prepared in lab, filtered through 0.2μ membrane filter in glass bottle and consumed within a maximum of 7 days.

6B.2.2 Preparation of Noopept loaded polymeric nanoparticles (NPT PNP)

Noopept loaded PNP was prepared using nanoprecipitation method. Briefly, the NPT and PLGA were dissolved in acetone. A 5 ml of Poloxamer 188 solution was prepared in prefiltered distilled water and continuously stirred on a magnetic stirrer at room temperature. Then organic phase was slowly added into aqueous phase using a 1ml syringe. The stirring was continued for next 3-4 hours to allow complete evaporation of organic solvent. The PNP dispersion was centrifuged for 10 minutes at 5000 rpm and 15°C for the sedimentation of free drug. The supernatant nanoparticulate dispersion was carefully separated without disturbing the free drug pellet at the bottom. The separated nanoparticulate dispersion was stored in glass vials at 2-8°C till further analysis.

6B.2.2.1 Establishing Quality target product profile (QTPP) and Critical Quality Attributes (CQA)

Based on the scientific, therapeutic, industrial and regulatory aspects, QTPP for NPT loaded polymeric nanoparticles were established. Further, based on the prior knowledge, literature review and experiment trials, three response variables viz., particle size, drug entrapment and drug loading were selected as CQA.

6B.2.2.2 Identification of Independent variables (factors) and qualitative risk assessment

Ishikawa diagram was used to demonstrate all the probable variables associated with development of NPT loaded PNP by nanoprecipitation method. These factors were qualitatively categorized as 'low, medium and high risk' based on their impact on CQA as described in Table 6B-1.

Table 6B-1. Quality risk assessment criteria

Low Risk	Factors with wide range of acceptability. No investigation required
Medium Risk	Acceptable risk. No adverse effect on product quality on small changes.
High Risk	Unacceptable risk. Acceptable range need to be investigated

Factors with low and medium risk were controlled by assigning constant levels based on literatures and preliminary trials.

6B.2.2.3 Quantitative risk assessment: Screening design

Factors with high risk were screened using 2-level fractional factorial design to statistically identify the critical factors and use them in main design to determine the control ranges (design space). Screening design was also utilized to assign constant levels of other non-critical factors. Minitab® 17.1.0 was used to generate a randomized design matrix based on which experimental batches were prepared and evaluated for CQA. Software based Pareto charts were utilized to determine critical factors while the main effect charts were utilized to decide the optimum levels of non-critical factors. Methods used for estimation of CQA are as follows

6B.2.2.3.1 Particle size and size distribution

Nanoparticulate dispersions were diluted ten times with pre-filtered distilled water, transferred to disposable sizing cuvette and analyzed by dynamic light scattering (DLS) using Nano-ZS Zetasizer, Malvern Instruments Ltd., UK for particle size (PS) and poly-dispersity index (PDI). The instrument analyzes angular scattering of a laser beam during its passage through the dispersed nanoparticulate sample and use the Mie theory of light scattering to calculate the mean diameter of nanoparticles.

6B.2.2.3.2 Drug entrapment and drug loading

Samples from nanoparticulate dispersions (0.1 ml) were dissolved and suitably diluted in acetonitrile and analyzed using HPLC method described in chapter 3. Drug entrapment (%) and drug loading (%) were then calculated using **Eq. 6B-1** and **Eq. 6B-2**.

$$\text{Drug entrapment}(\%) = \frac{\text{Entrapped drug (mg)}}{\text{Total drug taken (mg)}} \times 100 \qquad \text{Eq. 6B-1}$$

$$\text{Drug loading}(\%) = \frac{\text{Entrapped drug (mg)}}{\text{Total polymeric nanoparticles (mg)}} \times 100 \qquad \text{Eq. 6B-2}$$

6B.2.2.4 Formulation optimization by Box Behnken response surface design

Box-Behnken response surface design was applied to exhaustively investigate the relationship between critical factors and CQA with less number of experimental batches [4]. Minitab® 17.1.0 was used for generating the randomized design matrix and statistical evaluation of experimental data to achieve optimization solution and creating the design space. Suitability of model suggested by the software and identification of significant model terms were decided based on analysis of variance followed by F-test. Insignificant model terms were later removed to simplify the mathematical equations for calculation of CQA. The relationship between critical factors and CQA was explored using contour and 3-D response surface plots. Desirability criteria was defined based on QTPP and design space was created to obtain final optimized batch. Three batches were prepared with optimized composition for model verification.

6B.2.3 In-vitro characterization of optimized NPT PNP

6B.2.3.1 Shape and surface morphology

The NPT PNP (NPT loaded PNP with optimized composition) were evaluated for shape and surface characteristics using transmission electron microscopy. Dispersion was spread on a carbon-coated grid, excess solution was removed and the grid was dried under infrared lamp. It was negatively stained with 2% phosphotungstic acid (PTA) and again dried under Infrared lamp. Transmission electron microscope (CM 200, Philips, Netherlands) with operating voltage range of 20-200 kV was used to visualize nanoparticles at suitable enlargement with an accelerating voltage of 20 kV.

6B.2.3.2 Zeta potential

NPT PNP dispersion was diluted ten times with pre-filtered distilled water, transferred to disposable folded capillary cells and analyzed for zeta potential (ZP) using Nano-ZS zetasizer. The instrument utilizes Smoluchowski equation that calculates zeta potential based on amount of doppler shift occur due to electrophoretic mobility of colloidal particles in response to the electric field applied to the dispersion.

6B.2.3.3 In-vitro drug release study

The *in-vitro* drug release from optimized NPT PNP was evaluated using a Franz-type diffusion cell with an effective surface area of 3.14 cm^2 and a receptor chamber volume of 15 ml. Pre-activated dialysis membrane (MWCO, 12 kD) was mounted, as a permeation barrier, between donor and receptor chambers of diffusion cell. The receptor chamber was filled with a mixture of ethanol and double distilled water (ratio 3:7) as a diffusion media and allowed to equilibrate for half an hour. The optimized batches containing 1 mg of drug were transferred to donor chambers of diffusion cells. The diffusion medium was continuously stirred using a magnetic stirrer. 1 mL sample was withdrawn from sampling arm of diffusion cell at each time point up to 24 hours and equal volume of fresh diffusion media was added to maintain total receptor volume. Quantitative estimation of drug was performed using HPLC method at 258 nm detection wavelength as described earlier in Chapter 3. The kinetics of drug release was then evaluated by fitting the data in various mathematical models and comparing their regression coefficient (R^2) values [5].

6B.3. RESULTS & DISCUSSION

6B.3.1 Preparation and optimization of NPT loaded polymeric nanoparticles

6B.3.1.1 Establishing QTPP and CQA

Various QTPP elements and their targets were defined and presented with justification in Table 6B-2.

Table 6B-2. QTPP elements with justification for NPT loaded PNP

QTPP element		Target	Justification
Route of administration		Transdermal	Avoid first pass metabolism and achieve prolonged action
Dosage form		Polymeric nanoparticle	Better skin permeability and controlled drug release
Formulation quality attributes	Particle size#	Minimize (~100 nm)	To ensure better permeation and drug release
	Polydispersity Index	Minimize (< 0.3)	To ensure uniformity of size and related characteristics.
	Zeta potential	> ±30 mV	To ensure stability of the dispersion
	Surface characteristics	Spherical, smooth	To ensure better permeation
	Drug entrapment#	Maximize	To minimize drug wastage for cost-effectiveness
	Drug loading#	Maximize	For better drug release and less polymer exposure
	In vitro Drug release behavior	Prolonged for 24 hours	To ensure controlled drug release for desired duration
Ex vivo permeability		Better transdermal flux	To ensure PK/ PD comparable to marketed formulations
Stability		NLT 1 months	To ensure stability till incorporation in final dosage form
Safety		Non-toxic & Non-irritant to skin	To ensure safety of the final formulation
Pharmacokinetics		Similar or better than oral suspension	For bioequivalence requirement
Pharmacodynamics			To demonstrate therapeutic efficacy

Critical quality attributes

Particle size, drug entrapment and drug loading were identified as critical in governing the product quality and need to be within known limits to attain the pre-defined QTPP. Thus, these three characteristics were selected as CQA.

6B.3.1.2 Identification and qualitative assessment of Independent variables (factors)

All the probable variables associated with development of NPT loaded PNP by nanoprecipitation method were identified during the brainstorming sessions and categorized in to Material, Process, Equipment, Personnel and Environment. An ishikawa diagram illustrating

the cause and effect relationship among identified variables and CQA was constructed (**Fig. 6B-1**).

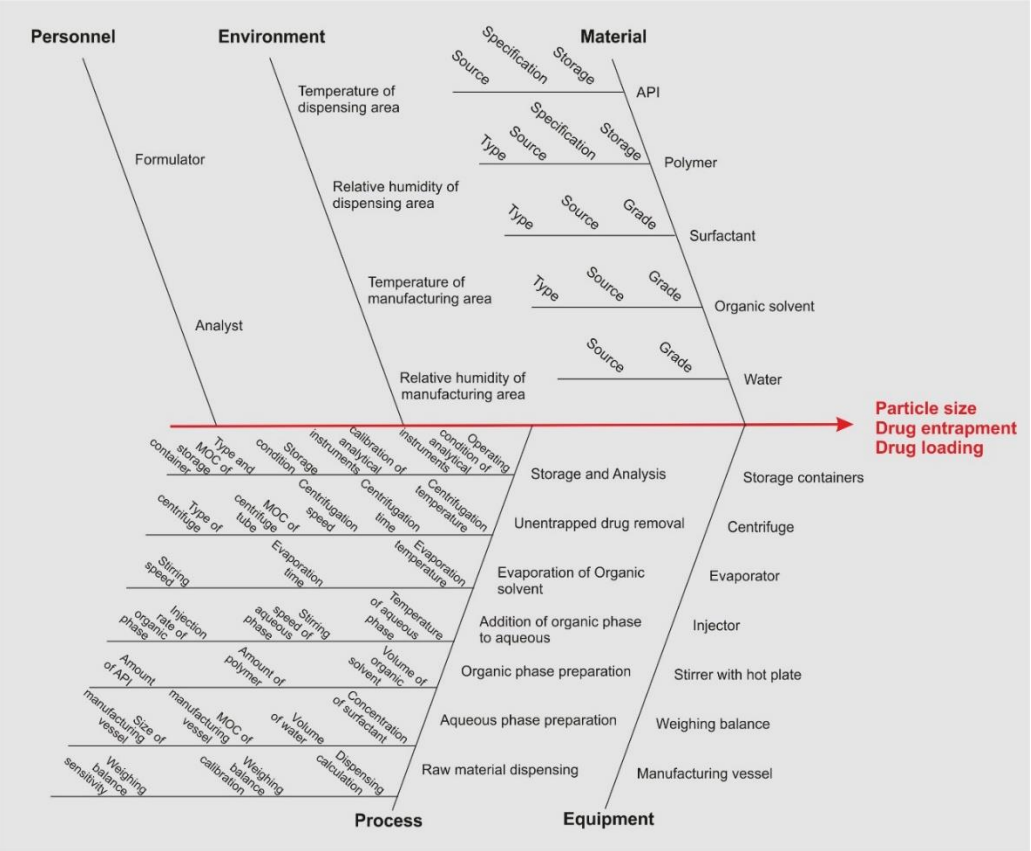

Fig. 6B-1. Ishikawa diagram showing probable variables that may influence the CQA

6B.3.1.3 Qualitative risk assessment

The risk associated with all the identified factors were evaluated based on the predefined criteria (**Table 6B-1**) and the result is presented in **Table 6B-3**. Factors with low and medium risk were assigned with the best available constant levels based on literature and preliminary trials to ensure no or negligible impact of these factors on CQA. These constant levels are also listed in **Table 6B-3**.

Table 6B-3. Qualitative risk assessment of independent variables

Factors	Process step	Impact on CQA	Constant levels
Source and specifications of API	Raw material Selection and Storage	Low risk	Authentic source with COA
Storage condition of API		Low risk	Stored at recommended condition
Type of Polymer		Low risk	PLGA 50:50
Source and specifications of Polymer		Low risk	Authentic source with COA

Factors	Process step	Impact on CQA	Constant levels
Storage condition of Polymer		Low risk	Stored at recommended condition
Type of Surfactant		Medium risk	Poloxamer 188
Source and specifications of Surfactant		Low risk	Authentic source
Storage condition of Surfactant		Low risk	Stored at recommended condition
Type of Organic solvent		Medium risk	Acetone
Source and specifications of Organic solvent		Low risk	Authentic source
Source of water		Low risk	In house
Grade of water		Low risk	Filtered (0.2µ) Double distilled
Weighing balance sensitivity	Dispensing	Low risk	0.1 mg
Weighing balance calibration		Low risk	Calibrated
Temperature and RH of Dispensing Area		Low risk	25±3°C, Ambient RH
Dispensing calculations		Low risk	Calculated using excel and verified
Type, Size and Material of Construction (MOC)	Manufacturing Vessel	Low risk	25 mL beaker of class A borosilicate glass
Temperature and Relative humidity	Manufacturing Area	Low risk	25±3°C, Ambient RH
Volume of Water	Aqueous phase preparation	Low risk	5 mL
Concentration of Surfactant		High risk	To be optimized
Amount of API	Organic phase preparation	High risk	To be optimized
Amount of Polymer		High risk	To be optimized
Volume of Organic solvent		High risk	To be optimized
Calibration of Injector and stirring equipment	Addition of Organic phase to aqueous	Low risk	Calibrated
Injection Rate of Organic phase		High risk	To be optimized
Stirring speed of Aqueous phase		High risk	To be optimized
Temperature of Aqueous phase		Low risk	Room temperature
Evaporation time	Evaporation of Organic solvent	Low risk	3-4 hours
Evaporation temperature		Low risk	Room temperature
Stirring speed during evaporation		Low risk	Same as used during organic phase addition
Type of Centrifuge		Low risk	Cooling centrifuge

Factors	Process step	Impact on CQA	Constant levels
Type and MOC of Centrifuge tube	Unentrapped drug removal	Low risk	15 mL conical-bottom glass tube with screw cap
Centrifugation speed		Medium risk	5000 rpm
Centrifugation time		Low risk	10 minutes
Centrifugation temperature		Low risk	15°C
Type and MOC of Storage container	Storage and Analysis	Low risk	20 mL flat-bottom glass vial with screw cap
Storage condition		Medium risk	2-8°C
Calibration of Analytical Instruments		Low risk	Calibrated
Methods used of Analysis		Low risk	Validated
Formulator	Personnel	Low risk	Common for all experiments and analysis
Analyst		Low risk	

Factors with high risk were carried forward for quantitative risk assessment.

6B.3.1.4 Quantitative risk assessment: Screening Design

Factors with high risk were statistically assessed by 2-level fractional factorial screening design. The low (-1) and high (+1) levels of all the independent variables were decided based on literatures as well as preliminary trials and are listed in **Table 6B-4**.

Table 6B-4. Various material attributes and process parameters along with their levels for screening by fractional factorial design

Independent variables		Unit	Levels	
			-1	+1
A:	Amount of Polymer (PLGA)	mg	20	40
B:	Amount of Drug (NPT)	mg	1.0	2.0
C:	Surfactant (Poloxamer 188) concentration	% w/v	0.25	0.50
D:	Rate of polymer addition	mL/min	0.5	1.0
E:	Stirring speed	rpm	500	1000
F:	Volume of organic solvent	mL	2	4

The randomized design matrix of 17 experimental batches (including one center point) was generated using Minitab® 17.1.0 statistical software and presented in **Table 6B-5**.

Table 6B-5. Randomized batch matrix and resulting CQA for screening design

Batch no.	Run order	Independent Variables						CQA		
		A	B	C	D	E	F	Particle Size (nm)	Drug Entrapment (%)	Drug loading (%)
S_1	05	-1	-1	-1	-1	-1	-1	105.9	82.44	4.12
S_2	06	+1	-1	-1	-1	+1	-1	110.2	73.60	1.84
S_3	13	-1	+1	-1	-1	+1	+1	77.1	72.38	7.24
S_4	12	+1	+1	-1	-1	-1	+1	112.4	81.39	4.07
S_5	02	-1	-1	+1	-1	+1	+1	79.5	88.56	4.43
S_6	04	+1	-1	+1	-1	-1	+1	117.8	76.52	1.91
S_7	11	-1	+1	+1	-1	-1	-1	106.3	68.32	6.83
S_8	17	+1	+1	+1	-1	+1	-1	130.6	74.26	3.71
S_9	10	-1	-1	-1	+1	-1	+1	87.7	92.20	4.61
S_{10}	15	+1	-1	-1	+1	+1	+1	104.3	79.21	1.98
S_{11}	07	-1	+1	-1	+1	+1	-1	92.4	67.06	6.71
S_{12}	09	+1	+1	-1	+1	-1	-1	133.9	70.21	3.51
S_{13}	14	-1	-1	+1	+1	+1	-1	97.4	84.23	4.21
S_{14}	03	+1	-1	+1	+1	-1	-1	119.1	75.53	1.89
S_{15}	08	-1	+1	+1	+1	-1	+1	95.3	61.01	6.10
S_{16}	16	+1	+1	+1	+1	+1	+1	100.7	77.29	3.86
S_{17}	01	0	0	0	0	0	0	106.8	78.80	3.94

The data were statistically processed by Minitab software to generate pareto, normal and main effect plots for all three CQA considering $P < 0.05$ as a level of significance.

Pareto and normal charts (**Fig. 6B-2**) clearly showed that polymer amount, stirring speed and volume of organic solvent had a significant effect on particle size of resulting nanoparticles. Amount of polymer as well as drug showed significant impact on drug loading. Similarly, amount of drug and its interactive effect with amount of polymer showed significant impact on drug entrapment. Owing to these observations, amount of polymer and amount of drug were selected as CMA while stirring speed and volume of organic solvent were selected as CPP for the final optimization step.

The influence of surfactant concentration and injection rate on the selected CQA was found insignificant. Hence, main effect plots were utilized to decide the constant level of these factors for final optimization step. Considering the positive impact on particle size and drug loading (**Fig. 6B-3**), lower levels of both the factors (surfactant concentration, 0.25 %w/v and injection rate, 0.5 mL/min) were chosen. Additionally,

selecting lower surfactant concentration might improve product safety via less surfactant exposure.

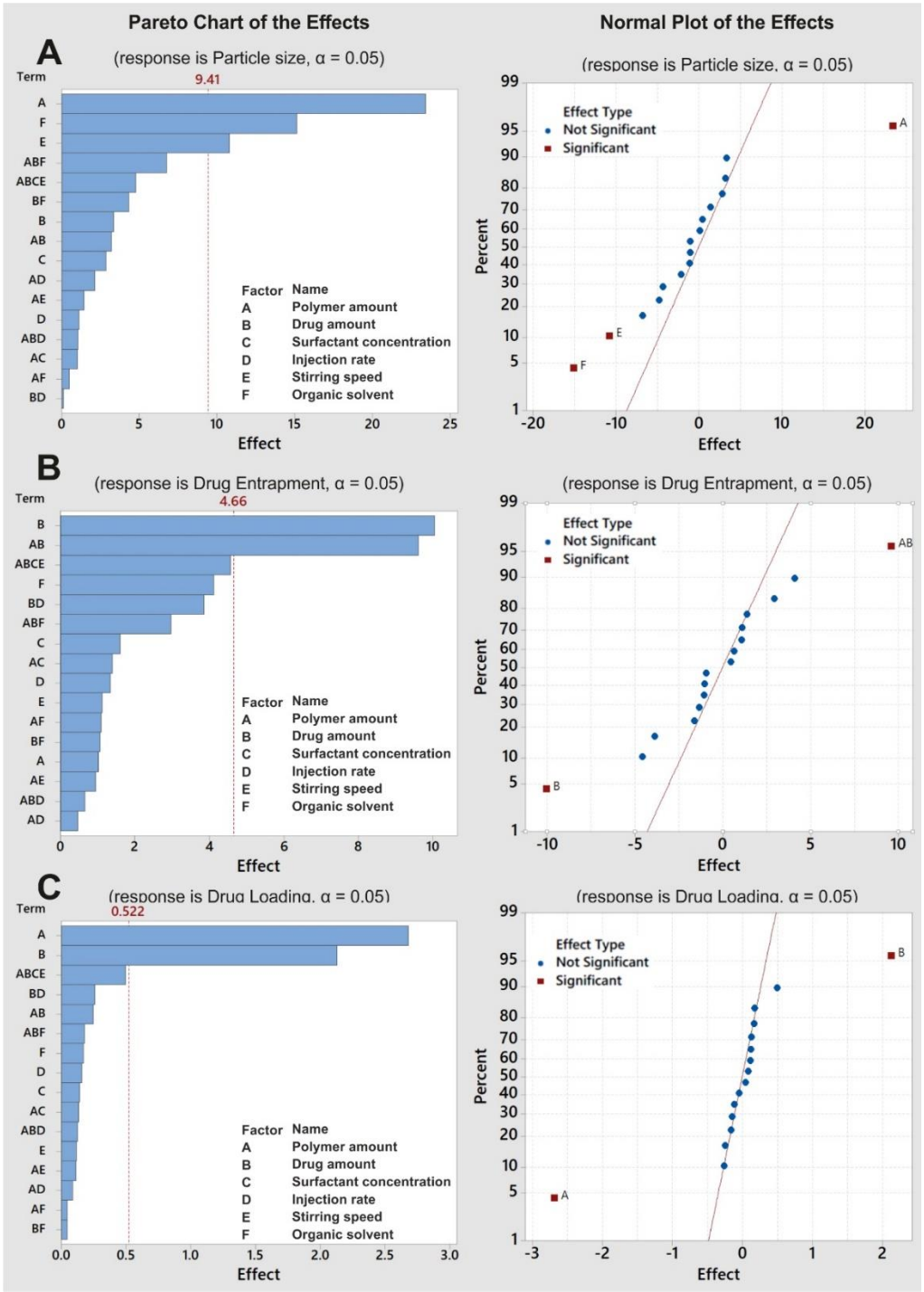

Fig. 6B-2. Pareto and Normal plots for A. Particle size, B. Drug entrapment and C. Drug loading

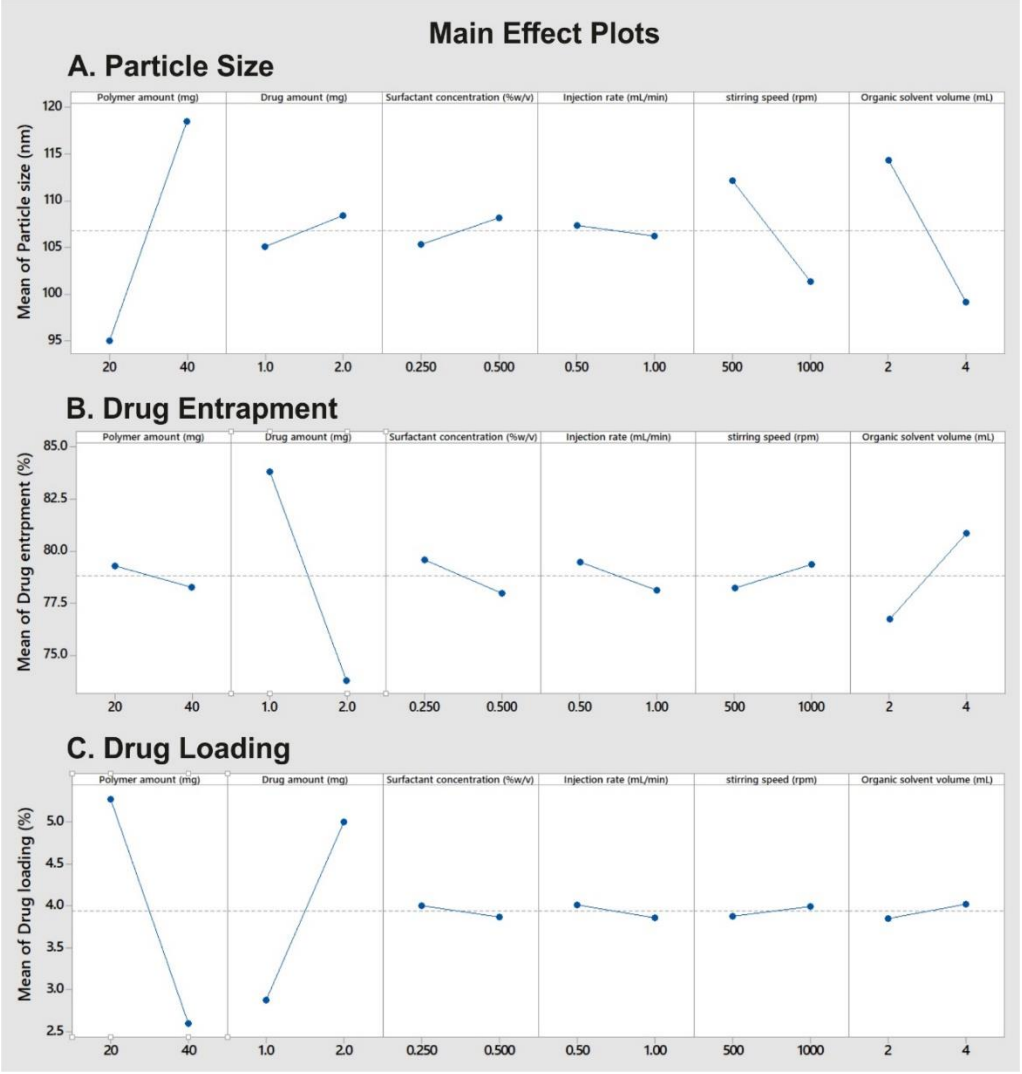

Fig. 6B-3. Main effect plots for A. Particle size, B. Drug entrapment and C. Drug loading

6B.3.1.5 Formulation optimization by Box Behnken response surface design

Based on the results of screening design, two CMA and two CPP were identified and their relationship with CQA were exhaustively investigated using Box-Behnken response surface design. Box-Behnken design was selected as it allows efficient estimation of quadratic terms with fewer design points that fall within safe operation limits as compared to central composite design [6]. The low (-1), medium (0) and high (+1) levels of all four CMA/CPP are listed in **Table 6B-6**.

Table 6B-6. Various critical material attributes and critical process parameters along with their levels for screening by Box-Behnken design

Independent variables (MAs/PPs)		Unit	Levels		
			-1	0	+1
A:	Amount of Polymer (PLGA)	mg	20	30	40
B:	Amount of Drug	mg	1.0	1.5	2.0
C:	Stirring speed	rpm	500	750	1000
D:	Volume of organic solvent	mL	2	3	4

A randomized matrix of twenty nine batches including five center points was generated by Minitab and presented in **Table 6B-7**. These batches were formulated as per their run order and evaluated for CQA using the methods described earlier. **Table 6B-7** also represents the resulting CQA of these batches.

Table 6B-7. Randomized design matrix for Box-Behnken response surface design

Batch no.	Run order	Independent Variables				CQA		
		A	B	C	D	Particle size (nm)	Drug entrapment (%)	Drug loading (%)
F_1	13	-1	-1	0	0	92.8	76.09	3.80
F_2	07	+1	-1	0	0	115.8	86.86	2.17
F_3	17	-1	+1	0	0	92.6	67.19	6.72
F_4	19	+1	+1	0	0	116.3	84.12	4.21
F_5	08	0	0	-1	-1	119.4	78.54	3.93
F_6	04	0	0	+1	-1	107.6	75.51	3.78
F_7	24	0	0	-1	+1	103.3	75.99	3.80
F_8	28	0	0	+1	+1	90.4	75.79	3.79
F_9	21	-1	0	0	-1	100.5	72.75	5.46
F_{10}	18	+1	0	0	-1	123.5	78.6	2.95
F_{11}	02	-1	0	0	+1	84.9	70.23	5.27
F_{12}	25	+1	0	0	+1	107.7	77.78	2.92
F_{13}	10	0	-1	-1	0	112	79.36	2.65
F_{14}	26	0	+1	-1	0	108.8	74.79	4.99
F_{15}	22	0	-1	+1	0	97.85	81.4	2.71
F_{16}	20	0	+1	+1	0	100.2	74.13	4.94
F_{17}	01	-1	0	-1	0	98.8	69.96	5.25
F_{18}	27	+1	0	-1	0	120.8	78.06	2.93
F_{19}	11	-1	0	+1	0	86.6	73.02	5.48
F_{20}	12	+1	0	+1	0	108.1	81.67	3.06
F_{21}	06	0	-1	0	-1	111.5	76.22	2.54
F_{22}	05	0	+1	0	-1	112.9	73.4	4.89
F_{23}	23	0	-1	0	+1	96.38	78.95	2.63
F_{24}	29	0	+1	0	+1	97.33	75.91	5.06
F_{25}	15	0	0	0	0	104.4	72.51	3.63

Batch no.	Run order	Independent Variables				CQA		
		A	B	C	D	Particle size (nm)	Drug entrapment (%)	Drug loading (%)
F_{26}	09	0	0	0	0	106.4	74.84	3.74
F_{27}	03	0	0	0	0	107.1	73.47	3.67
F_{28}	16	0	0	0	0	105.5	77.01	3.85
F_{29}	14	0	0	0	0	104.8	73.96	3.70

Analysis of variance (ANOVA) was performed by the software for full quadratic model consisting of Linear, quadratic and two-way interaction terms. Model terms with a p-value less than or equal to 0.05 (α-level) were considered as significant while terms with higher p-value were considered insignificant. Hierarchy based removal of insignificant model terms was done to simplify the model.

ANOVA and coded coefficients of Full as well as reduced quadratic model for particle size are presented in Table 6B-8 and Table 6B-9, respectively.

Table 6B-8. Analysis of variance of full as well as reduced quadratic model for particle size

Source	Full model					Reduced model (α out - 0.1)*				
	DF	Adj SS	Adj MS	F-Value	P-Value	DF	Adj SS	Adj MS	F-Value	P-Value
Model	14	2754.23	196.73	242.44	0	6	2751.06	458.51	694.53	0
Linear	4	2736.08	684.02	842.96	0	4	2736.08	684.02	1036.13	0
A	1	1541.33	1541.33	1899.47	0	1	1541.33	1541.33	2334.74	0
B	1	0.27	0.27	0.33	0.573	1	0.27	0.27	0.41	0.529
C	1	436.21	436.21	537.57	0	1	436.21	436.21	660.75	0
D	1	758.27	758.27	934.46	0	1	758.27	758.27	1148.6	0
Square	4	9.89	2.47	3.05	0.053	1	7.28	7.28	11.03	0.003
A^2	1	9.17	9.17	11.3	0.005	1	7.28	7.28	11.03	0.003
B^2	1	1.21	1.21	1.49	0.242					
C^2	1	1.67	1.67	2.06	0.173					
D^2	1	0.64	0.64	0.78	0.391					
2-Way Interaction	6	8.25	1.37	1.69	0.195	1	7.7	7.7	11.66	0.002
AB	1	0.12	0.12	0.15	0.703	1	7.7	7.7	11.66	0.002
AC	1	0.06	0.06	0.08	0.785					
AD	1	0.01	0.01	0.01	0.913					
BC	1	7.7	7.7	9.49	0.008					
BD	1	0.05	0.05	0.06	0.806					
CD	1	0.3	0.3	0.37	0.551					
Error	14	11.36	0.81			22	14.52	0.66		
Lack-of-Fit	10	6.39	0.64	0.51	0.821	18	9.55	0.53	0.43	0.906
Pure Error	4	4.97	1.24			4	4.97	1.24		
Total	28	2765.59				28	2765.59			

* Shaded rows represent insignificant model terms removed during model reduction

ANOVA table for particle size showed significant linear, quadratic and interaction effects. The p-value of individual model terms indicated a significant interaction among polymer amount and drug amount for particle size. Also, quadratic effect of polymer amount was found significant indicating that the relationship between polymer amount and particle size follow a curved line. Amount of polymer, stirring speed and volume of organic solvent were found to significantly influence the particle size. An insignificant lack-of fit showed the adequacy of the model in explaining the variation in the responses.

Table 6B-9. Coded coefficients of full as well as reduced quadratic model for particle size

Term	Full Model					Reduced model (α out - 0.1)*				
	Effect	Coef	SE Coef	T-Value	VIF	Effect	Coef	SE Coef	T-Value	VIF
Constant		105.64	0.403	262.23			105.051	0.197	533.08	
A	22.667	11.333	0.26	43.58	1	22.667	11.333	0.235	48.32	1
B	0.3	0.15	0.26	0.58	1	0.3	0.15	0.235	0.64	1
C	-12.058	-6.029	0.26	-23.19	1	-12.058	-6.029	0.235	-25.71	1
D	-15.898	-7.949	0.26	-30.57	1	-15.898	-7.949	0.235	-33.89	1
A^2	-2.378	-1.189	0.354	-3.36	1.08	-2.035	-1.017	0.306	-3.32	1
B^2	-0.863	-0.432	0.354	-1.22	1.08					
C^2	-1.016	-0.508	0.354	-1.44	1.08					
D^2	-0.626	-0.313	0.354	-0.88	1.08					
AB	0.35	0.175	0.45	0.39	1					
AC	-0.25	-0.125	0.45	-0.28	1					
AD	-0.1	-0.05	0.45	-0.11	1					
BC	2.775	1.388	0.45	3.08	1	2.775	1.388	0.406	3.42	1
BD	-0.225	-0.113	0.45	-0.25	1					
CD	-0.55	-0.275	0.45	-0.61	1					

* Shaded rows represent insignificant model terms removed during model reduction.

Coefficients table for particle size showed VIF values near to 1 indicating that the predictors are not correlated and regression coefficients are well estimated. Regression equations for full and reduced models in uncoded units are presented as **Eq. 6B-3** and **Eq. 6B-4**, respectively. The positive and negative sign before each coefficients indicates a direct or inverse relationship of that model term with particle size.

Full model

$$R1 = 100.2 + 1.847A - 3.22B - 0.0238C - 4.76D - 0.01189A^2 - 1.73B^2 - 0.000008C^2 - 0.313D^2 + 0.0350AB - 0.000050AC - 0.0050AD + 0.01110BC - 0.225BD - 0.00110CD$$

Eq. 6B-3

Reduced model

$$R1 = 115.87 + 1.744A - 8.03B - 0.04077C - 7.949D - 0.01017A^2 + 0.01110BC$$

Eq. 6B-4

ANOVA and coded coefficients of Full as well as reduced quadratic model for drug entrapment are presented in **Table 6B-10** and **Table 6B-11**, respectively.

Table 6B-10. Analysis of variance of full as well as reduced quadratic model for drug entrapment

Source	Full model					Reduced model (α out - 0.1)*				
	DF	Adj SS	Adj MS	F-Value	P-Value	DF	Adj SS	Adj MS	F-Value	P-Value
Model	14	408.5	29.179	5.06	0.002	3	381.42	127.14	29.48	0
Linear	4	352.569	88.142	15.29	0	2	350.62	175.311	40.65	0
A	1	278.885	278.885	48.37	0	1	278.89	278.885	64.67	0
B	1	71.736	71.736	12.44	0.003	1	71.74	71.736	16.64	0
C	1	1.936	1.936	0.34	0.571					
D	1	0.011	0.011	0	0.965					
Square	4	41.81	10.453	1.81	0.182	1	30.8	30.799	7.14	0.013
A^2	1	4.675	4.675	0.81	0.383					
B^2	1	36.132	36.132	6.27	0.025	1	30.8	30.799	7.14	0.013
C^2	1	7.638	7.638	1.32	0.269					
D^2	1	0.002	0.002	0	0.986					
2-Way Interaction	6	14.121	2.354	0.41	0.862					
AB	1	9.486	9.486	1.65	0.22					
AC	1	0.076	0.076	0.01	0.91					
AD	1	0.723	0.723	0.13	0.729					
BC	1	1.823	1.823	0.32	0.583					
BD	1	0.012	0.012	0	0.964					
CD	1	2.002	2.002	0.35	0.565					
Error	14	80.727	5.766			25	107.81	4.312		
Lack-of-Fit	10	69.1	6.91	2.38	0.21	21	96.18	4.58	1.58	0.357
Pure Error	4	11.627	2.907			4	11.63	2.907		
Total	28	489.228				28	489.23			

* Shaded rows represent insignificant model terms removed during model reduction

ANOVA table for drug entrapment showed significant quadratic and linear effects among selected CMA/CPP. Observing the individual terms showed that amount of polymer and amount of drug had significant linear effect on drug entrapment. Amount of drug also showed significant quadratic effect indicating that its relationship with particle size follow a curved line. An insignificant lack-of fit showed the adequacy of the model in explaining the variation in the responses.

Table 6B-11. Coded coefficients of full as well as reduced quadratic model for drug entrapment

Term	Full Model					Reduced model (α out - 0.1)*				
	Effect	Coef	SE Coef	T-Value	VIF	Effect	Coef	SE Coef	T-Value	VIF
Constant		74.36	1.07	69.24			75.276	0.504	149.46	
A	9.642	4.821	0.693	6.95	1	9.642	4.821	0.599	8.04	1
B	-4.89	-2.445	0.693	-3.53	1	-4.89	-2.445	0.599	-4.08	1
C	0.803	0.402	0.693	0.58	1					
D	-0.062	-0.031	0.693	-0.04	1					

Term	Full Model					Reduced model (α out - 0.1)*				
	Effect	Coef	SE Coef	T-Value	VIF	Effect	Coef	SE Coef	T-Value	VIF
A^2	1.698	0.849	0.943	0.9	1.08					
B^2	4.72	2.36	0.943	2.5	1.08	4.185	2.092	0.783	2.67	1
C^2	2.17	1.085	0.943	1.15	1.08					
D^2	0.033	0.016	0.943	0.02	1.08					
AB	3.08	1.54	1.2	1.28	1					
AC	0.27	0.14	1.2	0.11	1					
AD	0.85	0.43	1.2	0.35	1					
BC	-1.35	-0.68	1.2	-0.56	1					
BD	-0.11	-0.06	1.2	-0.05	1					
CD	1.42	0.71	1.2	0.59	1					

* Shaded rows represent insignificant model terms removed during model reduction

Coefficients table for drug entrapment showed VIF values near to 1 indicating that the predictors are not correlated and regression coefficients are well estimated. Regression equations for full and reduced models in uncoded units are presented as **Eq. 6B-5** and **Eq. 6B-6**, respectively. The positive and negative sign before each coefficients indicates a direct or inverse relationship of that model term with drug entrapment.

Full model

$$R2 = 123.6 - 0.658A - 38.1B - 0.0265C - 3.36D + 0.00849A^2 + 9.44B^2 + 0.000017C^2 + 0.016D^2 + 0.308AB + 0.000055AC + 0.043AD - 0.00540BC - 0.11BD + 0.00283CD$$

Eq. 6B-5

Reduced model

$$R2 = 86.98 + 0.4821A - 30.00B + 8.37B^2$$

Eq. 6B-6

ANOVA and coded coefficients of Full as well as reduced quadratic model for drug loading are presented in **Table 6B-12** and **Table 6B-13**, respectively.

Table 6B-12. Analysis of variance of full as well as reduced quadratic model for drug loading

Source	Full model					Reduced model (α out - 0.1)*				
	DF	Adj SS	Adj MS	F-Value	P-Value	DF	Adj SS	Adj MS	F-Value	P-Value
Model	14	34.1575	2.4398	174.05	0	4	34.0982	8.5245	800.42	0
Linear	4	32.7753	8.1938	584.51	0	2	32.7706	16.3853	1538.51	0
A	1	15.7297	15.7297	1122.08	0	1	15.7297	15.7297	1476.96	0
B	1	17.0408	17.0408	1215.61	0	1	17.0408	17.0408	1600.07	0
C	1	0.0043	0.0043	0.31	0.588					
D	1	0.0005	0.0005	0.03	0.858					
Square	4	1.1705	0.2926	20.87	0	1	1.134	1.134	106.48	0
A^2	1	1.1453	1.1453	81.7	0	1	1.134	1.134	106.48	0
B^2	1	0.0227	0.0227	1.62	0.224					
C^2	1	0.0206	0.0206	1.47	0.245					
D^2	1	0.0028	0.0028	0.2	0.664					

Source	Full model					Reduced model (α out - 0.1)*				
	DF	Adj SS	Adj MS	F-Value	P-Value	DF	Adj SS	Adj MS	F-Value	P-Value
2-Way Interaction	6	0.2117	0.0353	2.52	0.073	1	0.1936	0.1936	18.18	0
AB	1	0.1936	0.1936	13.81	0.002	1	0.1936	0.1936	18.18	0
AC	1	0.0022	0.0022	0.16	0.697					
AD	1	0.0063	0.0063	0.45	0.515					
BC	1	0.0031	0.0031	0.22	0.644					
BD	1	0.0015	0.0015	0.1	0.752					
CD	1	0.005	0.005	0.36	0.56					
Error	14	0.1963	0.014			24	0.2556	0.0107		
Lack-of-Fit	10	0.1672	0.0167	2.3	0.219	20	0.2265	0.0113	1.56	0.361
Pure Error	4	0.0291	0.0073			4	0.0291	0.0073		
Total	28	34.3538				28	34.3538			

* Shaded rows represent insignificant model terms removed during model reduction

ANOVA table for drug loading showed significant quadratic, interaction and linear effects. The p-value of individual model terms indicated a significant linear as well as interaction effect of polymer amount and drug amount for particle size. Also, quadratic effect of polymer amount was found significant indicating that the relationship between polymer amount and particle size follow a curved line. An insignificant lack-of fit showed the adequacy of the model in explaining the variation in the responses.

Table 6B-13. Coded coefficients of full as well as reduced quadratic model for drug loading

Term	Full Model					Reduced model (α out - 0.1)*				
	Effect	Coef	SE Coef	T-Value	VIF	Effect	Coef	SE Coef	T-Value	VIF
Constant		3.7179	0.0529	70.22			3.782	0.025	151.1	
A	-2.2898	-1.1449	0.0342	-33.5	1	-2.2898	-1.1449	0.0298	-38.43	1
B	2.3833	1.1917	0.0342	34.87	1	2.3833	1.1917	0.0298	40	1
C	0.0379	0.0189	0.0342	0.55	1					
D	-0.0125	-0.0062	0.0342	-0.18	1					
A^2	0.8404	0.4202	0.0465	9.04	1.08	0.803	0.4015	0.0389	10.32	1
B^2	0.1184	0.0592	0.0465	1.27	1.08					
C^2	0.1128	0.0564	0.0465	1.21	1.08					
D^2	0.0413	0.0206	0.0465	0.44	1.08					
AB	-0.44	-0.22	0.0592	-3.72	1	-0.44	-0.22	0.0516	-4.26	1
AC	-0.0471	-0.0235	0.0592	-0.4	1					
AD	0.0791	0.0396	0.0592	0.67	1					
BC	-0.056	-0.028	0.0592	-0.47	1					
BD	0.0382	0.0191	0.0592	0.32	1					
CD	0.0707	0.0354	0.0592	0.6	1					

* Shaded rows represent insignificant model terms removed during model reduction

Coefficients table for drug loading showed VIF values near to 1 indicating that the predictors are not correlated and regression coefficients are well estimated. Regression equations for full and reduced models in

uncoded units are presented as **Eq. 6B-7** and **Eq. 6B-8**, respectively. The positive and negative sign before each coefficients indicates a direct or inverse relationship of that model term with drug entrapment.

Full model

$$R3 = 6.95 - 0.3054A + 3.047B - 0.00108C - 0.412D + 0.004202A^2 + 0.237B^2 + 0.000001C^2 + 0.0206D^2 - 0.0440AB - 0.000009AC + 0.00396AD - 0.000224BC + 0.038BD + 0.000141CD$$

Eq. 6B-7

Reduced model

$$R3 = 5.275 - 0.2894A + 3.703B + 0.004015A^2 - 0.0440AB$$

Eq. 6B-8

Model summary for all the three CQA is presented in **Table 6B-14**. A low S value and high R^2 value indicated a better prediction of responses by the model. Predicted R^2 was found to be in good agreement with other R^2 further supporting the prediction potential of the model.

Table 6B-14. Summary of full as well as reduced quadratic model for all three CQA

Responses	Full model				Reduced model (α out - 0.1)			
	S	R-sq	R-sq (adj)	R-sq (pred)	S	R-sq	R-sq (adj)	R-sq (pred)
Particle size (nm)	0.900808	99.59	99.18	98.39	0.81251	99.47	99.33	99.14
Drug entrapment (%)	2.4013	83.50	67.00	14.93	2.0766	77.96	75.32	68.11
Drug loading (%)	0.118399	99.43	98.86	97.06	0.103199	99.26	99.13	98.54

Four different residual plots viz., normal probability plot, residual versus fitted values, histogram and residual versus order of data were generated for all three CQA and presented in **Fig. 6B-4**. In normal probability graph, residuals were appeared to follow a straight line indicating that the data was normally distributed. Residual versus fitted values graph and residual versus order of data graph showed random scattering of residuals around zero indicating a constant variance and uncorrelated error, respectively.

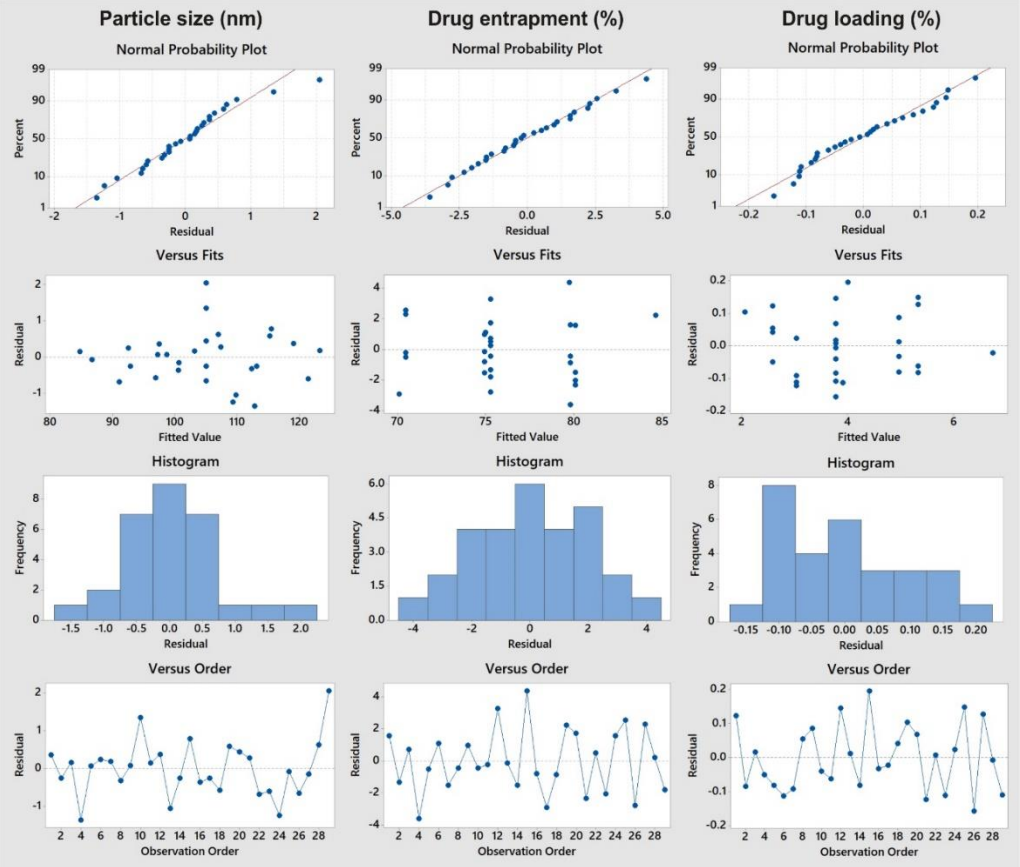

Fig. 6B-4. Residual plots for all three CQA

The main effect plots for all three CQA are presented in **Fig. 6B-5**. These graphs provided a better depiction of how the individual CMA/CPP influence respective CQA and found in-line with the ANOVA results.

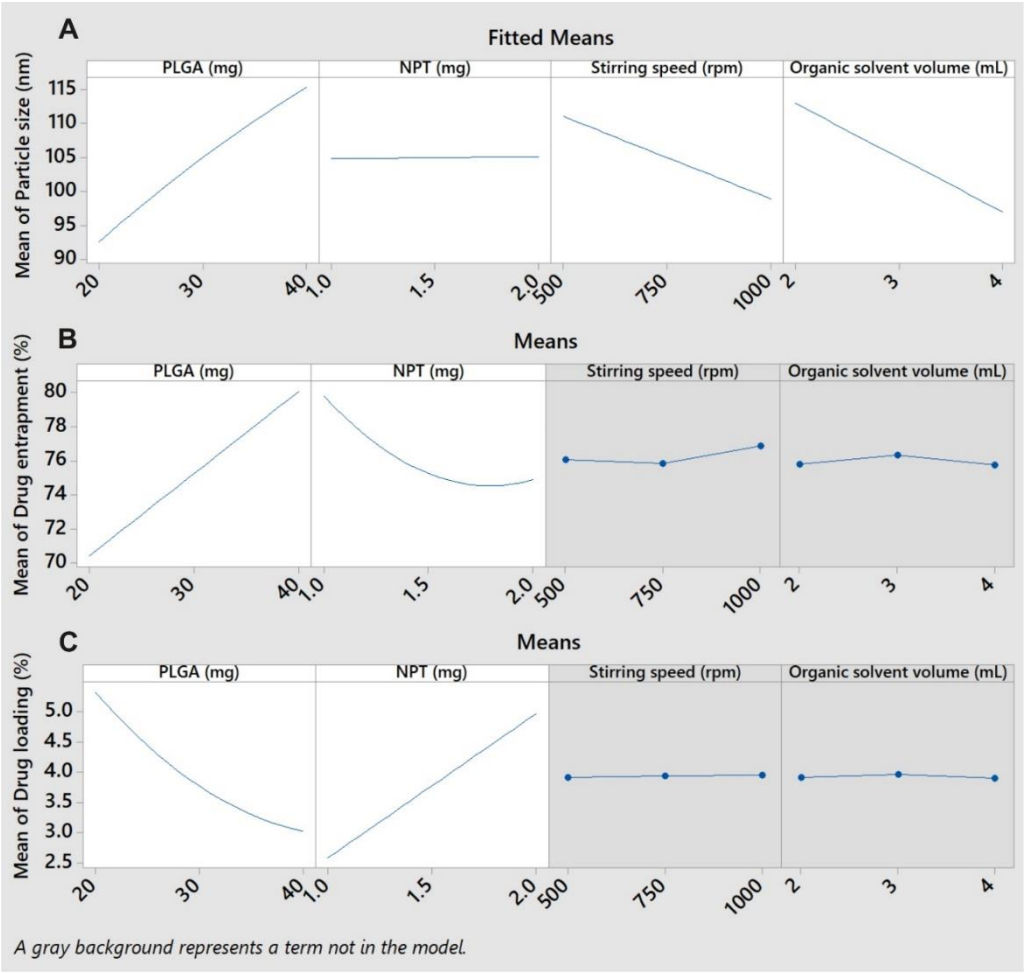

Fig. 6B-5. Main effect plots of reduced quadratic model for A. particle size, B. drug entrapment and C. drug loading

Contour and response surface plots are presented in **Fig. 6B-6** and **Fig. 6B-7**, respectively. These graphs were used to depict how the CQA is related to any two CMA/CPP while keeping other CMA/CPP at constant (mid) levels.

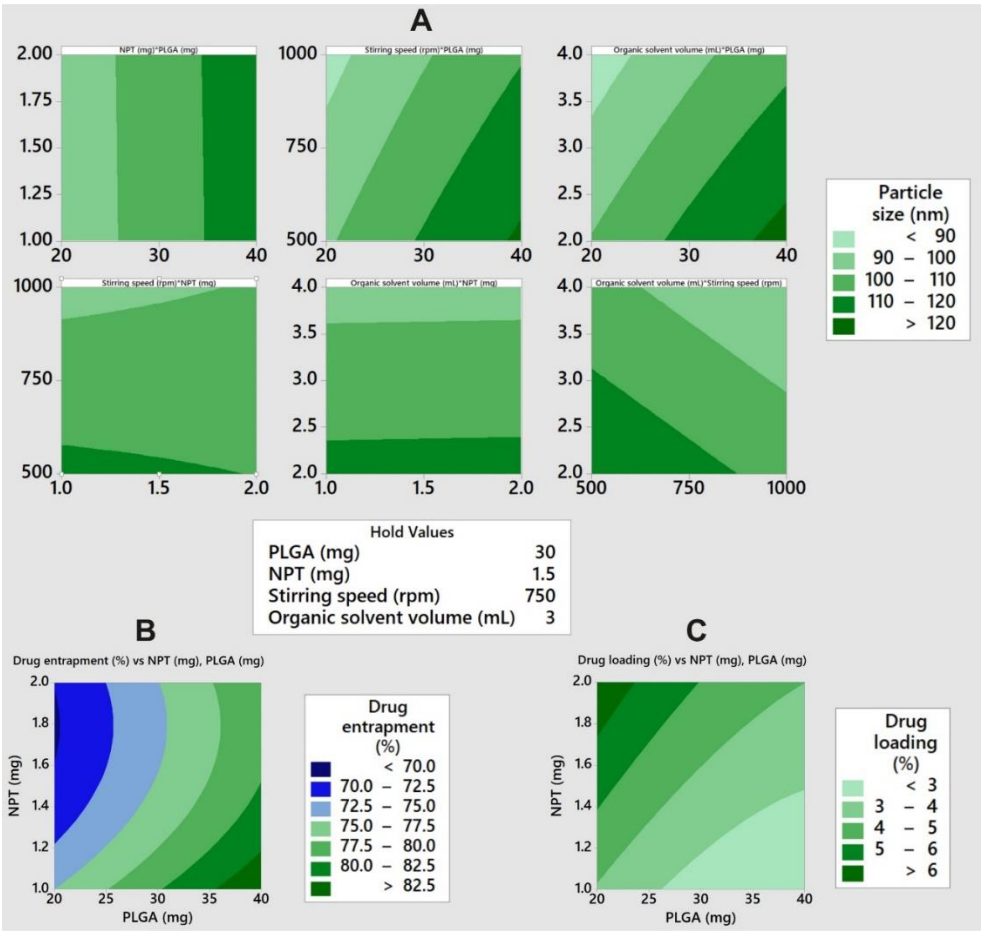

Fig. 6B-6. Contour plots of reduced quadratic model for A. particle size, B. drug entrapment and C. drug loading

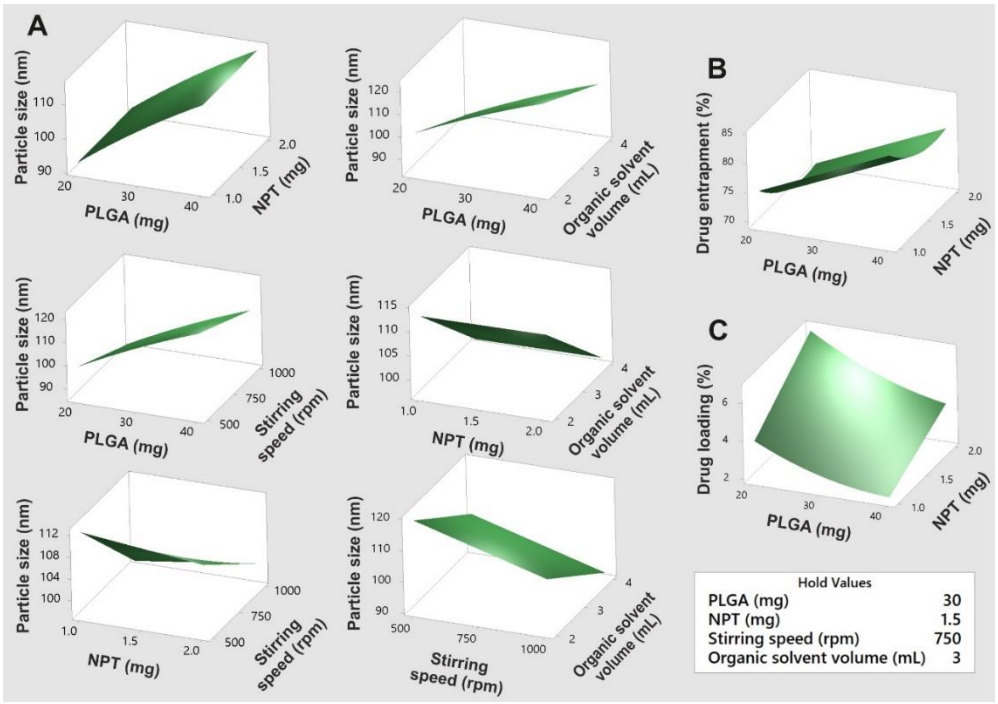

Fig. 6B-7. Response surface plots of reduced quadratic model for A. particle size, B. drug entrapment and C. drug loading

Table 6B-15. Criteria for optimization of NPT PNP

Responses	Goal	Lower	Target	Upper	Weight	Importance
Particle size (nm)	Minimum	84.9	-	123.5	1	1
Drug entrapment (%)	Target	67.19	70	86.86	1	1
Drug loading (%)	Maximum	2.1715	-	6.719	1	1

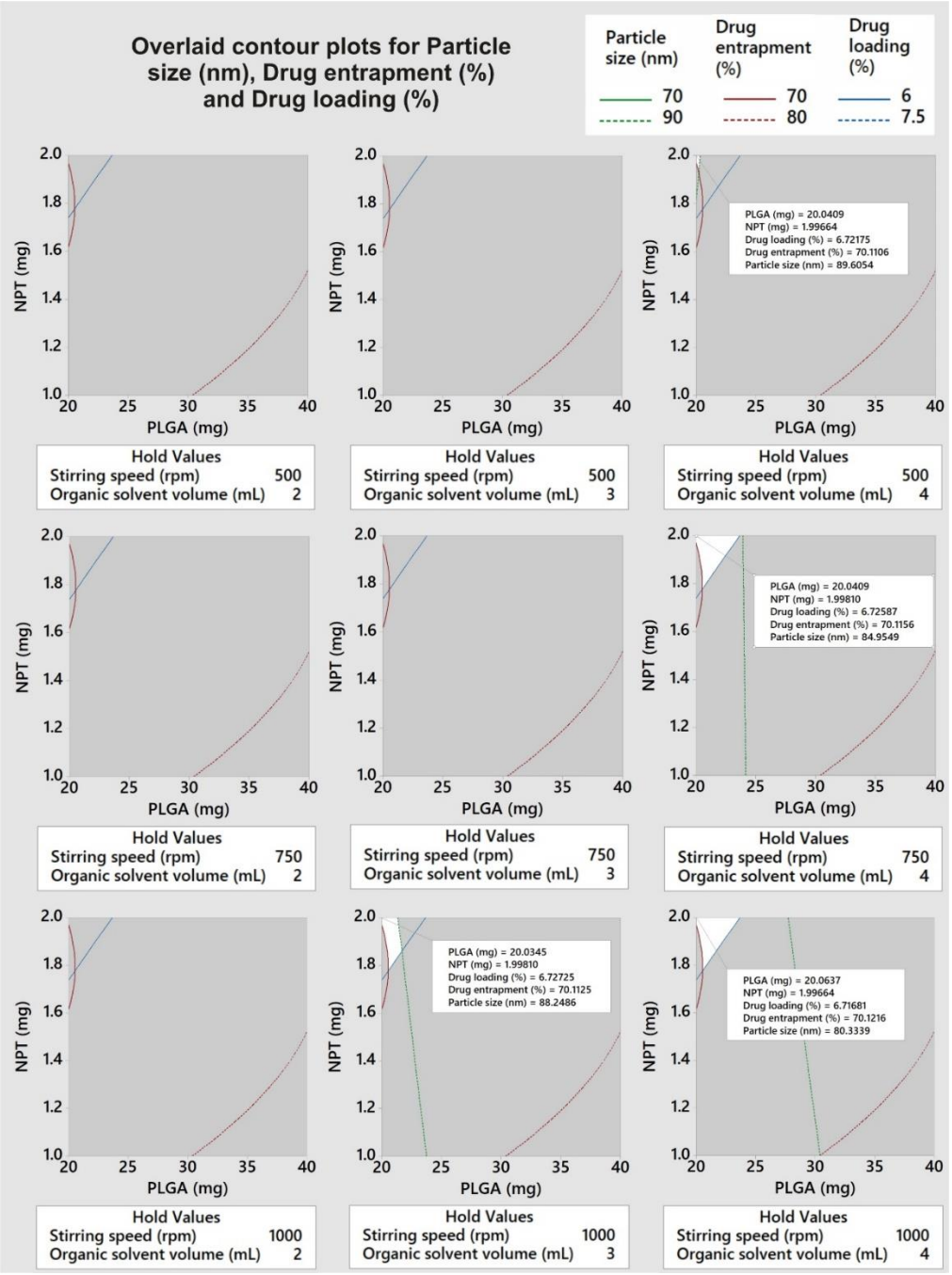

Fig. 6B-8. Overlaid contour plots of reduced quadratic model with higher and lower range of all three CQA showing design space

Overlaid contour plots for all three CQA were generated for their desirable range (**Fig. 6B-8**) to observe the design space (white area in graph). The overlaid plot between PLGA and NPT at 1000 rpm stirring

speed and 4 mL organic solvent volume, showed a design space with largest area with lowest particle size at lower PLGA and higher NPT amount. Further, the response optimizer plot was generated using the criteria shown in **Table 6B-15**. The target for drug entrapment was set at 70% to maximize the drug loading which was desirable for better drug release and to reduce polymer exposure.

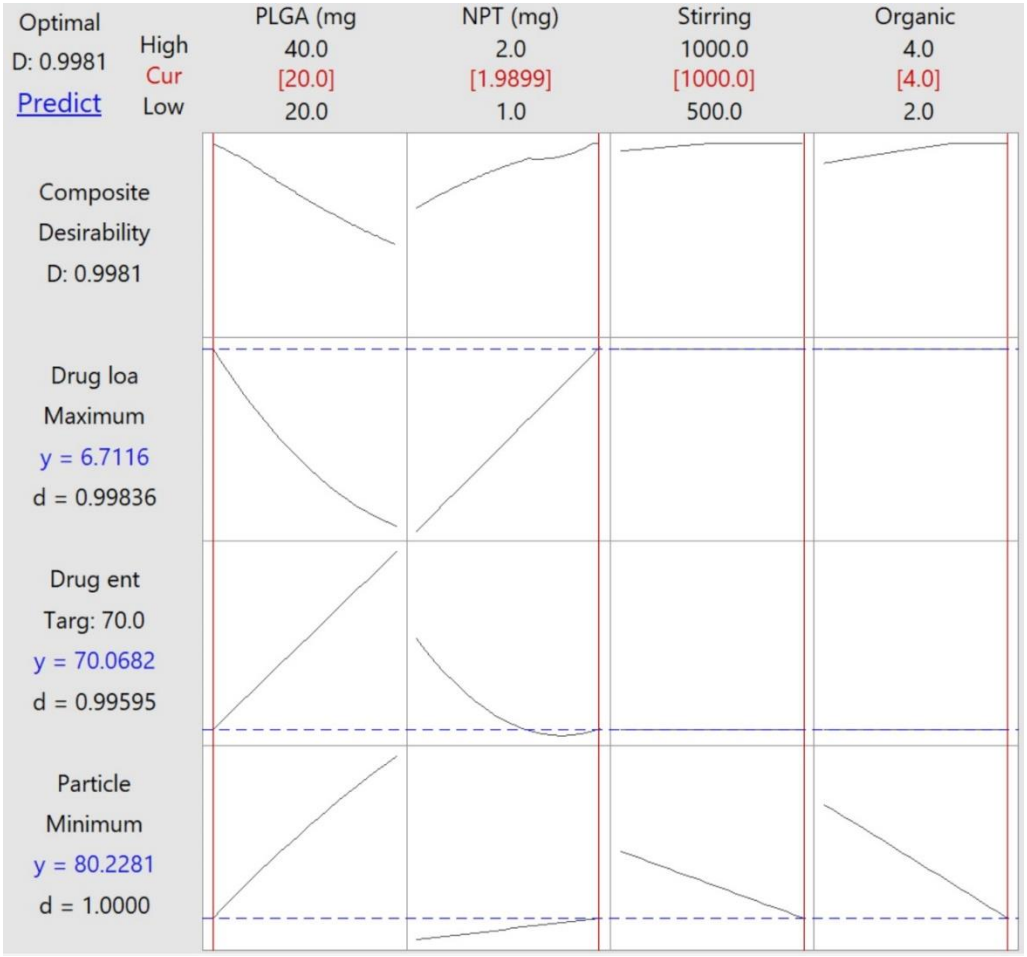

Fig. 6B-9. Response optimizer plot showing individual and composite desirability of predicted optimum levels

The response optimizer plot showed an optimization solution having a composite desirability of 0.9981. the setting of this optimization solution is also presented in **Table 6B-16** along with the 95% confidence as well as 95% prediction intervals. Three batches with optimized levels were prepared for verification trials and the values of different CQA are presented in **Table 6B-17**.

Table 6B-16. Optimization solution

Multiple Response Prediction

Variable	Setting
PLGA (mg)	20
NPT (mg)	2
Stirring speed (rpm)	1000
Organic solvent volume (mL)	4

Responses	Fit	SE Fit	95% Confidence interval		95% Prediction interval	
			Lower	Upper	Lower	Upper
Particle size (nm)	80.228	0.657	78.87	81.59	78.06	82.4
Drug entrapment (%)	70.07	1.02	67.97	72.16	65.31	74.83
Drug loading (%)	6.7116	0.072	6.56	6.86	6.45	6.97

Table 6B-17. Results of verification trials

Responses	95% Prediction interval		Results			
	Lower	Upper	Batch-1	Batch-2	Batch-3	Average
Particle size (nm)	78.06	82.4	79.07	82.17	80.55	80.60
Drug entrapment (%)	65.31	74.83	68.64	71.48	72.07	70.73
Drug loading (%)	6.45	6.97	6.65	6.62	6.70	6.66

The average values of all three CQA were found to fall within 95% confidence interval and thus indicated the validity of the model.

6B.3.2 In-vitro characterization of optimized NPT PNP

6B.3.2.1 Shape and surface morphology

Transmission electron microscopy of optimized NPT PNP was performed and the image is represented as **Fig. 6B-10**. The image showed spherical shape with smooth surface of nanoparticles. The size of nanoparticles seen in the image was found in-line with the results of particle size data obtained from Malvern zetasizer (**Fig. 6B-11**).

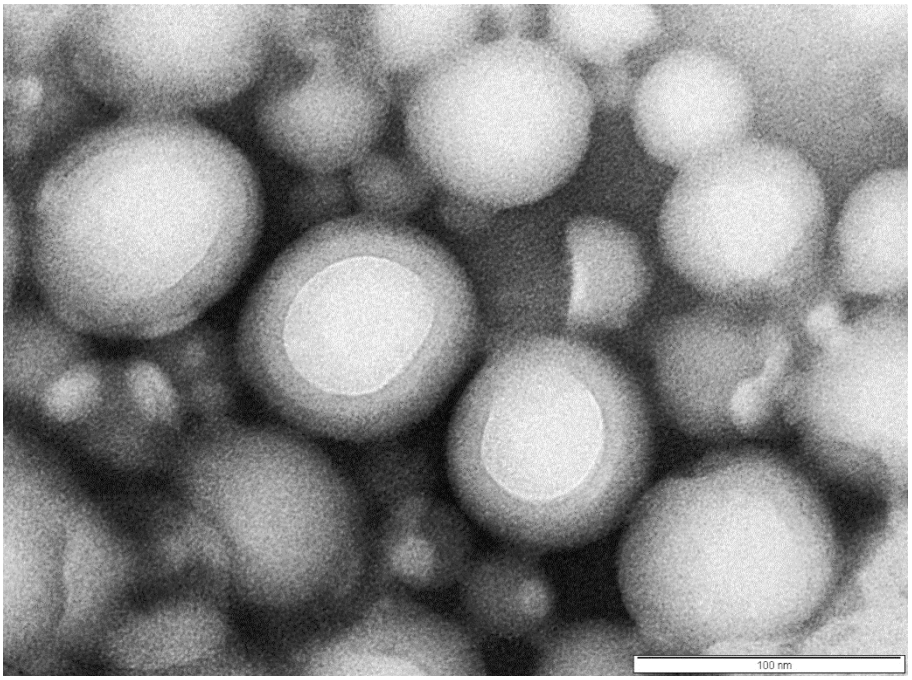

Fig. 6B-10. Transmission electron microscopic image of optimized NPT PNP

System

Temperature (°C):	25.0	**Duration Used (s):**	70
Count Rate (kcps):	202.9	**Measurement Position (mm):**	4.65
Cell Description:	Disposable sizing cuvette	**Attenuator:**	6

Results

			Size (r.nm):	% Intensity	Width (r.nm):
Z-Average (r.nm):	79.07	**Peak 1:**	83.36	100.0	23.18
PdI:	0.084	**Peak 2:**	0.000	0.0	0.000
Intercept:	0.959	**Peak 3:**	0.000	0.0	0.000

Result quality : Good

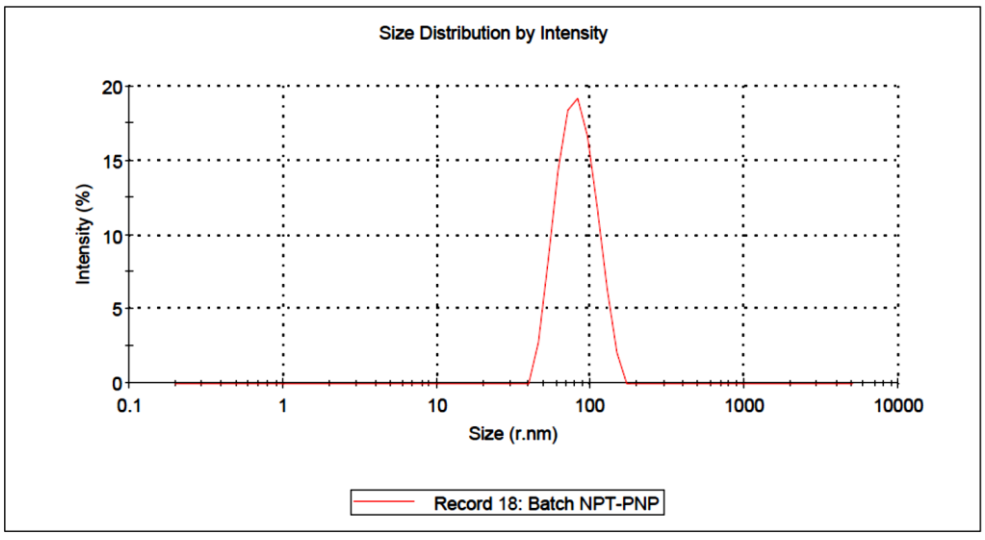

Fig. 6B-11. Size distribution graph of optimized NPT PNP

6B.3.2.2 Zeta potential

The zeta potential graph of optimized NPT PNP (**Fig. 6B-12**) showed a net negative charge on nanoparticle surface with a zeta potential value of -36.5 mV. The charge was found sufficient enough to keep the particles dispersed via repulsive forces [7, 8].

System

Temperature (°C):	25.0	**Zeta Runs:**	12
Count Rate (kcps):	227.7	**Measurement Position (mm):**	2.00
Cell Description:	Clear disposable zeta cell	**Attenuator:**	8

Results

		Mean (mV)	Area (%)	Width (mV)
Zeta Potential (mV):	-36.5	**Peak 1:** -36.5	100.0	5.39
Zeta Deviation (mV):	5.39	**Peak 2:** 0.00	0.0	0.00
Conductivity (mS/cm):	0.0194	**Peak 3:** 0.00	0.0	0.00

Result quality : Good

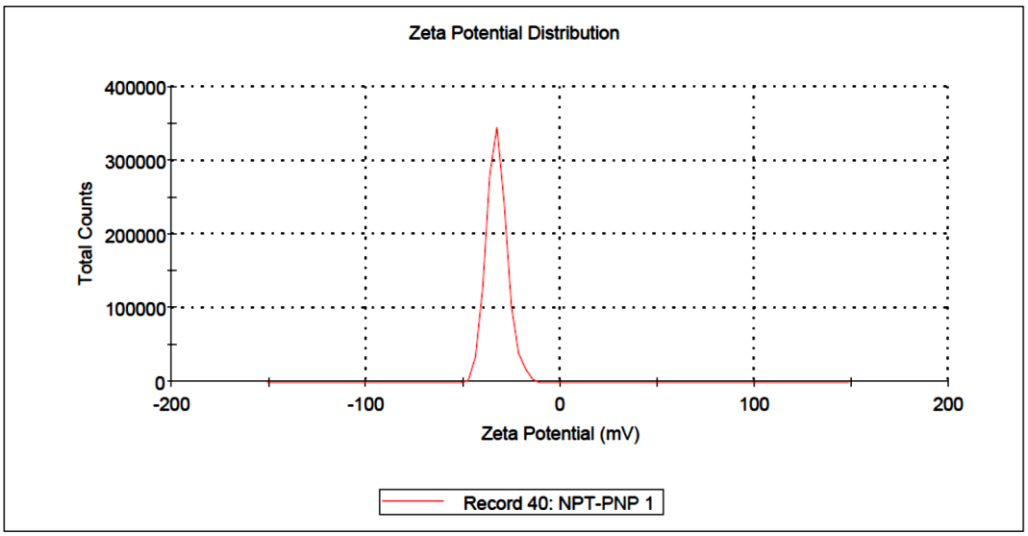

Fig. 6B-12. Zeta potential graph of optimized NPT PNP

6B.3.2.3 In-vitro drug release study

In vitro drug release from NPT PNP was evaluated and the cumulative percent drug release at different time points are summarized in **Table 6B-18** as well as illustrated in **Fig. 6B-13**. In order to ensure that the presence of NPT in release media directly reflects its release from nanocarriers, the permeation of released NPT across dialysis membrane should not be rate limiting. Hence, data for NPT solution was also generated which showed >90% drug release within 2 hours indicating non-barrier nature of dialysis membrane for dissolved NPT. Release data

of NPT PNP showed >50 % NPT release in first 8 hours and > 80 % release in 24 hours indicating the control release behavior of PNP.

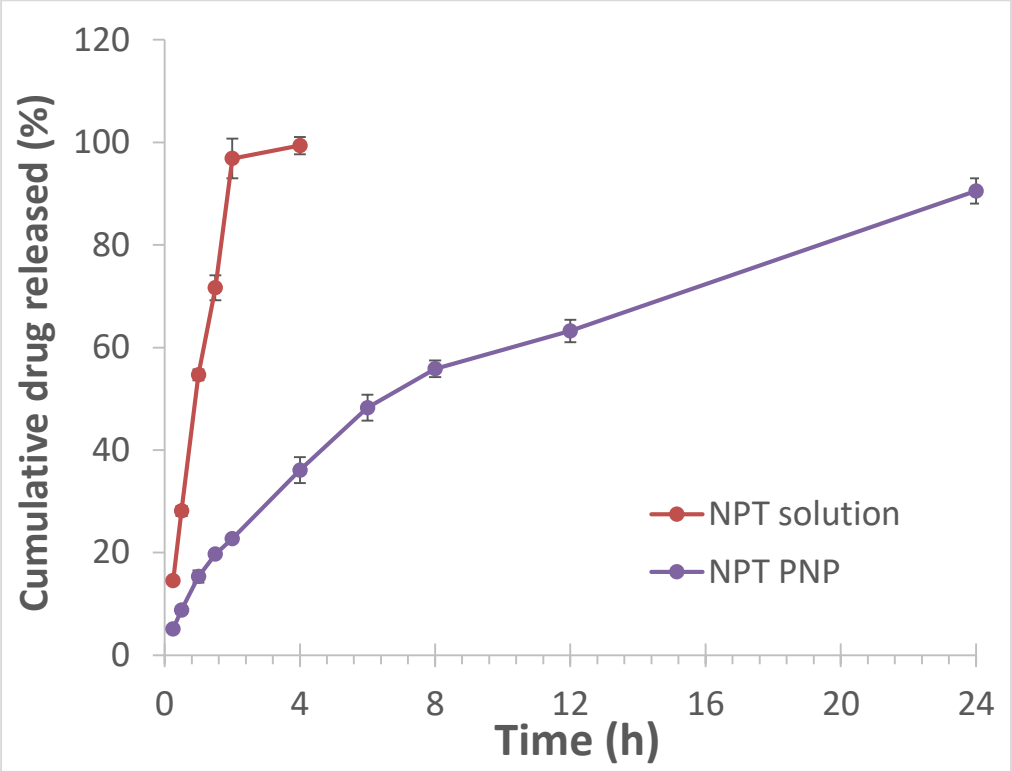

Fig. 6B-13. Cumulative percent of NPT released *in vitro* versus time curve for PNP

Table 6B-18. *In vitro* release profile of NPT from its solution and PNP

Time (h)	Cumulative percent drug released	
	NPT Solution*	NPT PNP*
0.25	14.52 ± 0.48	5.13 ± 0.23
0.5	28.12 ± 0.96	8.81 ± 0.69
1	54.66 ± 1.05	15.34 ± 1.19
1.5	71.63 ± 2.46	19.71 ± 0.42
2	96.84 ± 3.85	22.73 ± 0.56
4	99.36 ± 1.70	36.09 ± 2.55
6	-	48.25 ± 2.54
8	-	55.83 ± 1.62
12	-	63.22 ± 2.17
24	-	90.50 ± 2.49

* Result represented as mean ± SD

The result of various mathematical models, applied to understand the NPT release kinetics from PNP, are presented in **Table 6B-19**.

Table 6B-19. Various mathematical models and their correlation coefficient values

Mathematical models	Graph description (Y-axis versus X-axis)	NPT PNP	
		R^2	n
Zero order	Cumulative amount/percent of drug released *versus* time	0.951	-

Mathematical models	Graph description (Y-axis versus X-axis)	NPT PNP	
		R^2	n
First order	Log cumulative percent drug remaining *versus* time	-0.996	-
Higuchi	Cumulative percent drug released *versus* square root of time	0.997	-
Hixon Crowell	Cube root of percent drug remaining *versus* time	-0.993	-
Korsmeyer Peppas	Log cumulative percent drug released *versus* log time	0.995	0.66

The R^2 values for Higuchi as well as first order model was found higher suggesting a diffusion controlled system where release rate is dependent on remaining drug concentration within the carrier.

REFERENCES

1. Santander-Ortega, M., et al., *Nanoparticles made from novel starch derivatives for transdermal drug delivery.* Journal of controlled release, 2010. **141**(1): p. 85-92.
2. Barichello, J.M., et al., *Encapsulation of hydrophilic and lipophilic drugs in PLGA nanoparticles by the nanoprecipitation method.* Drug development and industrial pharmacy, 1999. **25**(4): p. 471-476.
3. Lawrence, X.Y., *Pharmaceutical quality by design: product and process development, understanding, and control.* Pharmaceutical research, 2008. **25**(4): p. 781-791.
4. Eriksson, L., et al., *Design of experiments.* Principles and Applications, Learn ways AB, Stockholm, 2000.
5. Quinn, H.L., et al., *Design of a Dissolving Microneedle Platform for Transdermal Delivery of a Fixed-Dose Combination of Cardiovascular Drugs.* J Pharm Sci, 2015. **104**(10): p. 3490-500.
6. *Minitab StatGuide, Minitab 17 Statistical Software*. 2010, Minitab, Inc.: State College, PA.
7. *Zeta potential: An introduction in 30 minutes*. Zetasizer Nano series technical note 2017 [cited 2017; Available from: https://www.materials-talks.com/wp-content/uploads/2017/09/mrk654-01_an_introduction_to_zeta_potential_v3.pdf.
8. Salopek, B., D. Krasic, and S. Filipovic, *Measurement and application of zeta-potential.* Rudarsko-geolosko-naftni zbornik, 1992. **4**(1): p. 147.